Abstract

Title of Document: DESIGNING HYDROGELS THAT TRANSFORM THEIR SHAPE IN RESPONSE TO MOLECULAR CUES

Jasmin C. Athas, Doctor of Philosophy, 2016

Dissertation directed by: Professor Srinivasa R. Raghavan

Department of Chemical and Biomolecular Engineering

There has been considerable interest in developing shape-changing soft materials for potential applications in drug delivery, microfluidics and biosensing. These shape-changing materials are inspired by the morphological changes exhibited by plants in nature, such as the Venus flytrap. One specific class of shape-change is that from a flat sheet to a folded structure (e.g., a tube). Such "self-folding" materials are usually composed of polymer hydrogels, and these typically fold in response to external stimuli such as pH and temperature. In order to develop these hydrogels for the previously described applications, it is necessary to expand the range of triggers. The focus of this dissertation is the advancement of shape-changing polymer hydrogels that are sensitive to uncommon cues such as specific biomolecules (enzymes), the substrates for such enzymes, or specific multivalent cations.

First, we describe a hybrid gel that responds to the presence of low concentrations of a class of enzymes known as matrix metalloproteinases (MMPs). The hybrid gel was created by utilizing photolithographic techniques to combine two or more gels with distinct chemical composition into the same material. Certain portions of the hybrid gel

are composed of a biopolymer derivative with crosslinkable groups. The hybrid gel is flat in water; however, in the presence of MMPs, the regions containing the biopolymer are degraded and the flat sheet folds to form a 3D structure. We demonstrate that hydrogels with different patterns can transform into different 3D structures such as tubes, helices and pancakes. Furthermore, this shape change can be made to occur at physiological concentrations of enzymes.

Next, we report a gel with two layers that undergoes a shape change in the presence of glucose. The enzyme glucose oxidase (GOx) is immobilized in one of the layers. GOx catalyzes the conversion of glucose to gluconic acid. The production of gluconic acid decreases the local pH. The decrease in local pH causes one of the layers to swell. As a result, the flat sheet folds to form a tube. The tube unfolds to form a flat sheet when it is transferred to a solution with no glucose present. Therefore, this biomolecule-triggered shape transformation is reversible, meaning the glucose sensing gel is reusable. Furthermore, this shape change only occurs in the presence of glucose and it does not occur in the presence of other small sugars such as fructose.

In our final study, we report the shape change of a gel with two layers in the presence of multivalent ions such as Ca^{2+} and Sr^{2+}. The gel consists of a passive layer and an active layer. The passive layer is composed of dimethylyacrylamide (DMAA), which does not interact with multivalent ions. The active layer consists of DMAA and the biopolymer alginate. In the presence of Ca^{2+} ions, the alginate chains crosslink and the active layer shrinks. As a result, the gel converts from a flat sheet to a folded tube. What

is particularly unusual is the direction of folding. In most cases, when flat rectangular gels fold, they do so about their short-side. However, our gels typically fold about their long-side. We hypothesize that non-homogeneous swelling determines the folding axis.

DESIGNING HYDROGELS THAT TRANSFORM THEIR SHAPE IN RESPONSE TO MOLECULAR CUES

by

Jasmin C. Athas

Dissertation submitted to the Faculty of the Graduate School of the

University of Maryland, College Park, in partial fulfillment of

the requirements for the degree of

Doctor of Philosophy

2016

Advisory Committee:

Prof. Srinivasa Raghavan, Chair

Professor Lyle Isaacs

Professor Jeffrey Davis

Professor Sang Bok Lee

Professor Ian White

Acknowledgements

First, I would like to thank Professor Raghavan for his support and mentoring throughout my graduate studies. As my advisor, he encouraged me to explore several research areas. I learnt the art of story telling through the critical arrangement of figures and data and to present my research to a wide audience. He taught me to ask the right questions and challenge assumptions. For all this, I am truly grateful.

I would also like to thank my committee: Professor White, Professor Isaacs, Professor Lee and Professor Davis for their advice and suggestions. I am grateful to the following undergraduate students: Kelly Jun, Caitlyn McCafferty, Catherine Nguyen and Shailaa Kummar for their help with experiments.

I am grateful to my group members, both past and present. It has been a great pleasure to work with them. In particular, I would like to thank Dr. Bani Cipriano, Dr. Joe White, Dr. Chanda Arya, Kevin Diehn, Ankit Gargava, Annie Lu, Kerry DeMella and Brady Zarket for their valuable insight and companionship.

This would not have been possible without the help, love, support and encouragement that I have received from friends and family. Pat, thank you for valuable advice and support. I thank Ammi for instilling in me a love for science and encouraging me to pursue my dreams. You have always been my cheerleader. Thathi, you have inspired me to work hard and with integrity. I appreciate all your hard work. I also thank Seeya for encouraging me to be curious and perseverant. I would like to deeply thank

Bhuvan for his unwavering support and encouragement throughout this endeavor. I appreciate for your feedback, and help. I look forward to our future together.

Table of Contents

List of Figures

Abbreviations

AAm	Acrylamide
BIS	N,N'-Methylenebisacrlyamide
DMAA	Dimethylacrylamide
DMAEMA	2-(Dimethylamino)ethyl methacrylate
EGDMA	Ethylene glycol dimethacrylate
GOx	Glucose Oxidase
Lap	Laponite
LCST	Lower Critical Solution Temperature
MMP	Matrix metalloproteinase
NIPA	N-Isopropylacrylamide
PEGDA	Poly(ethyleneglycol) diacrylate
PEGDMA	Poly(ethylene glycol) dimethacrlyate

Chapter 1

Introduction and Overview

1.1 Problem Description and Motivation

Structures in nature frequently exhibit changes in their shape. Two examples of plants that demonstrate rapid shape-transformations are the Venus flytrap and the mimosa. These changes are driven by a change in swelling ratio (i.e. turgor pressure) between different layers of plant tissue. Fibrous plant tissue consists of rigid cellulose fibers embedded in a soft, swellable matrix.[1,2] The direction of this shape transformation is determined by the orientation of the cellulose fibers. The swelling of plant tissue takes place in the direction that is perpendicular to the direction of the cellulose fibers. The reversible movements of plants are discussed in further detail in Section 2.4.

While many man-made actuators rely heavily on electricity and pneumatics to trigger a shape transformation, recently researchers have drawn inspiration from these plants and have designed actuators that change shape in response to differential changes in swelling between their components. Polymer hydrogels are the materials of choice in these applications. Hydrogels are three-dimensional polymer networks that imbibe large amounts of water.[3,4] Stimuli-responsive hydrogels have the ability to undergo a drastic change in swelling ratio in response to an external stimulus such as pH or temperature.[5,6] Another advantage of hydrogels is their similarity in "softness" to materials in nature such as squids and jellyfish.

Hydrogels with multiple layers have been commonly utilized to create shape changing structures.[7-10] The general approach involves combining layers of hydrogels with different swelling properties in order to achieve a shape response. A bilayer consists of one layer that swells to a greater degree (the active layer) and the second layer that swells to a lower extent or undergoes no swelling (the passive layer). Inhomogeneous swelling leads to the creation of non-uniform stresses at the boundary between the two layers.[11,12] As a result, the flat hydrogel sheet releases these stresses by folding. Furthermore, the swelling properties of the active and passive layers can be tuned to tailor the shape response.[8] These structures have potential applications in microfluidics,[13] drug delivery[10,14] and biosensing.[15] For instance, a bilayer hydrogel structure can be used as a valve to control the liquid flow in a microchannel. A change in the solution composition would cause the active layer to swell and thereby block the flow.

With respect to the use of polymer hydrogels to mimic shape-changing biomaterials, there are two areas with significant opportunity for advancement. First, while there are several reports of hydrogels undergoing a shape transformation in response to stimuli such as pH and temperature, the range of triggers needs to be expanded in order to widen applications.[16,17] For instance, it is of interest to prepare structures that respond to the presence of a specific biomolecule. Biomolecular reactions are highly specific, i.e they occur in a lock-key manner.[18] Also, at the cellular level, very low concentrations (~ nanomolar) of biomolecules are adequate to induce substantial responses.[18,19] Thus, a goal is to make gels that similarly respond (by changing shape) to very low concentrations of biomolecules. Such gels could be useful in applications such

as biosensing and drug delivery. A second area for further research is in unusual shape changes. For instance, in rectangular hydrogels, folding commonly occurs along the short axis as opposed to the long axis of the sheet.[11,19,20] An ability to control the axis of folding could be useful for future applications.

1.2 Proposed Approach

In this dissertation, we introduce three new concepts for shape-changing (folding) of hydrogels: folding induced by an enzyme; folding induced by the substrate for an enzyme (glucose); and folding induced by multivalent ions.

1.2.1 Enzyme-Triggered Folding of Hydrogels

The goal of our first study (Chapter 3) was to fabricate a hydrogel sheet that undergoes a macroscopic change in response to the presence of miniscule concentrations of a specific biomolecule. Towards this end, we report a hydrogel film that responds to a class of enzymes called matrix metalloproteinases (MMPs). Our gel is a hybrid of three different constituents arranged in a specific pattern using photolithography. Initially, the sheet is flat when placed in water. When collagenase, a type of MMP, is added to the water, the enzyme cleaves the chains in one of the gel layers. As a result, the swollen outer layer is able to fold over the softer inner layer, causing the sheet to transform into a specific shape such as a folded tube (Figure 1.1). The kinetics of the folding transition are dependent on the concentration of the enzyme. Furthermore, these gels are capable of responding to the physiological concentrations of MMPs present in cell lysate. We also demonstrate the versatility of our technique by utilizing different patterns to create a range of 3D structures including tubes, helices and pancakes. Furthermore, we

demonstrate that this hybrid film can be utilized as a hinge in a larger structure; specifically, we used it to create an analog of the Venus flytrap.

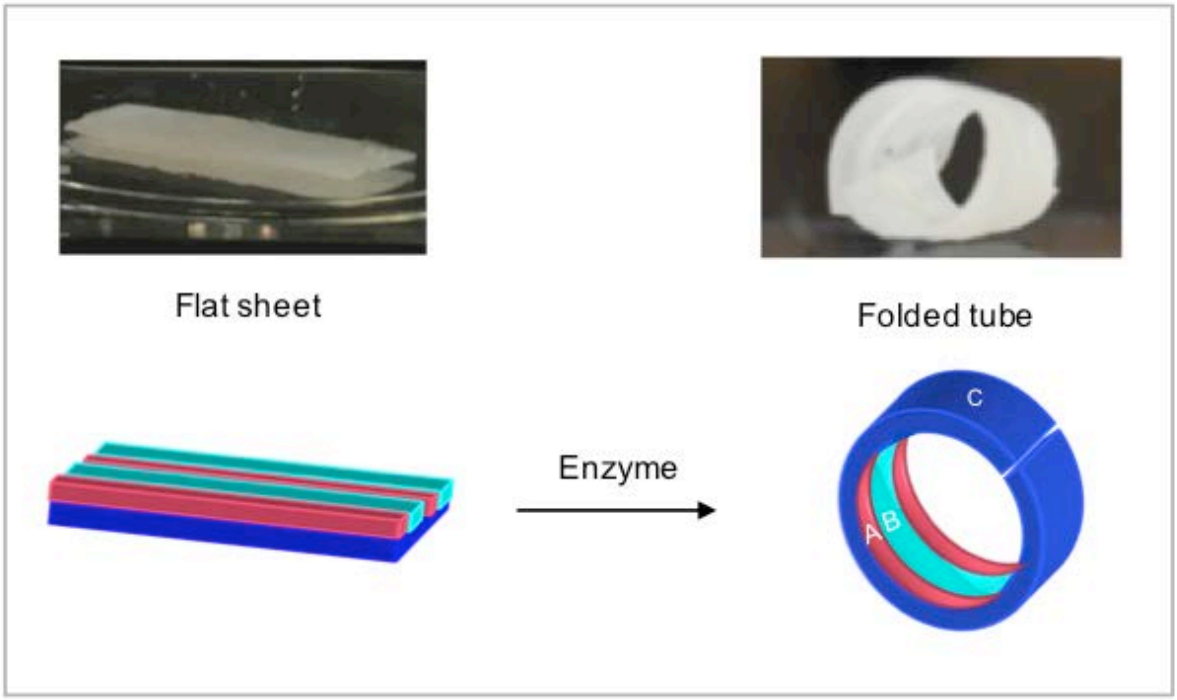

Figure 1.1. Enzyme triggered folding of hydrogels described in Chapter 3.

1.2.2 Glucose-Triggered Folding of Hydrogels

In Chapter 4, we present a hybrid hydrogel that responds to the substrate for an enzymatic reaction (glucose). Our gel has two layers, with one passive layer containing the enzyme, glucose oxidase. This enzyme catalyzes the oxidation of glucose to gluconic acid in the presence of oxygen. The production of gluconic acid leads to a drop in pH, which causes the active layer to undergo a dramatic increase in swelling. This leads to differential stresses, which causes the flat hydrogel sheet to fold into a closed tube (Figure 1.2). The kinetics of folding are dependent on the concentration of glucose. This folding behavior is also reversible i.e. the gel unfolds in water and refolds in the presence

of glucose. Furthermore, as a proof of concept, we demonstrate that this folding behavior can be used to distinguish between glucose and other sweeteners in solution.

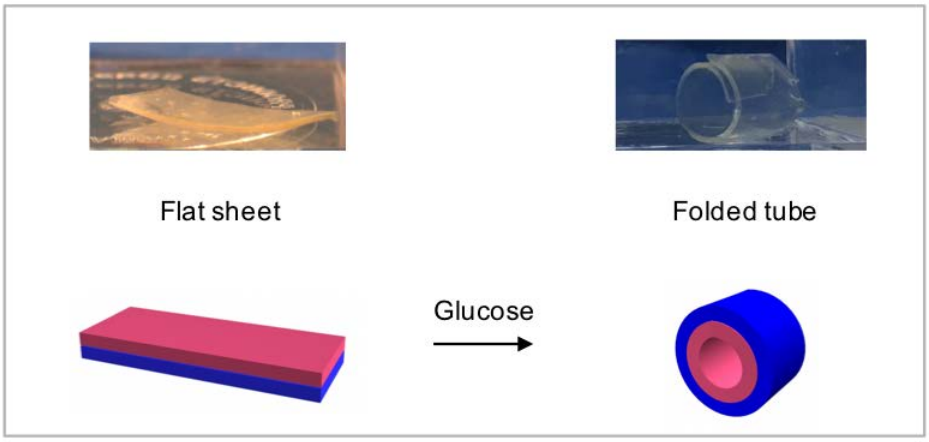

Figure 1.2. Glucose triggered folding of hydrogels described in Chapter 4.

1.2.3 Multivalent Cation-Triggered Folding of Hydrogels

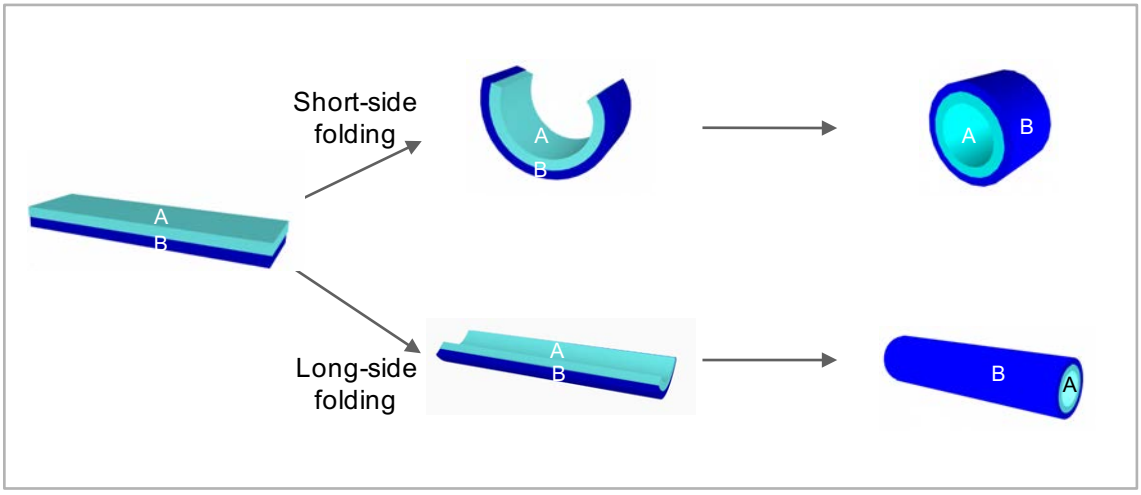

Figure 1.3. Folding behavior of bilayer hydrogels described in Chapter 5.

Our last study is on the unusual folding of certain gels having two layers, one passive, and the other containing the biopolymer alginate. It is well known that alginate solutions undergo crosslinking and gelation in the presence of multivalent ions such as

Ca^{2+}, Ba^{2+} or Fe^{3+}. We find that the addition of these ions causes the flat gel to fold to form a tube. While previous reports have found that folding of gel sheets generally occurs only along the short axis,[11,20] we demonstrate that by controlling different parameters such as the concentration of ions, the folding can be made to occur along the long axis (Figure 1.3). This is an unexpected and novel result. We observe that the concentration of ion affects the direction of folding.

1.3 Significance of This Work

The significance of this work is twofold: first, the creation of new hydrogels that undergo shape changes upon addition of specific molecules (enzymes, substrates, ions), and the second, the insights gained into such folding. Biomolecule-induced shape changes could be used to expand the applications for such gels in biosensing and drug delivery. For example, the levels of enzymes, including matrix metalloproteinases (MMPs), change after injury and during diseases such as cancer and rheumatoid arthritis.[19,21] Thus, gels that are responsive to MMPs could be used to trigger a macroscopic response to disease or injury in the body. Similarly, glucose-sensitive gels can be used to detect the type of sweetener used in beverages. Finally, our study on gel folding due to cations demonstrates several variables that affect the direction of folding. The insight gained from this study can be applied to other systems to direct folding along specific directions. Finally, it is worth noting that the raw materials used to fabricate our hydrogels are inexpensive and widely available, thereby allowing our work to be accessible to other researchers. We anticipate that the new directions we set forth in this field will be further investigated and will lead to practical applications.

Chapter 2

Background

2.1 Hydrogels

Hydrogels are three-dimensional polymer networks containing water in the interstitial spaces.[3,4] The polymer chains are crosslinked by chemical or physical bonds.[3,4] Chemically crosslinked hydrogels have permanent junctions (i.e. covalent crosslinks). Physical bonds refer to interactions such as ionic interactions, hydrogen bonds or hydrophobic interactions.

Hydrogels are commonly synthesized by free-radical polymerization of a monomer and crosslinker in water. Figure 2.1 demonstrates the mechanism behind free-radical polymerization for a monomer, NIPA and a tetrafunctional crosslinker, N,N-methylene bisacrylamide (MBAA). Irgacure 2959, i.e., 1-[4-(2-hydroxyethoxy)-phenyl]-2-hydroxy-2-methyl-1-propanone is the free-radical initiator. In the presence of UV light at the appropriate wavelength (~ 280 nm), Irgacure 2959 is cleaved to form free radicals.[22] The free radicals add to a monomer molecule and open the double bond to form a new radical. This process continues as more monomers are added to the growing polymer chain. Since BIS is bifunctional, it reacts with two such chains and forms crosslinks. The reaction terminates when all the radicals have reacted or all the monomer and crosslinker are consumed.

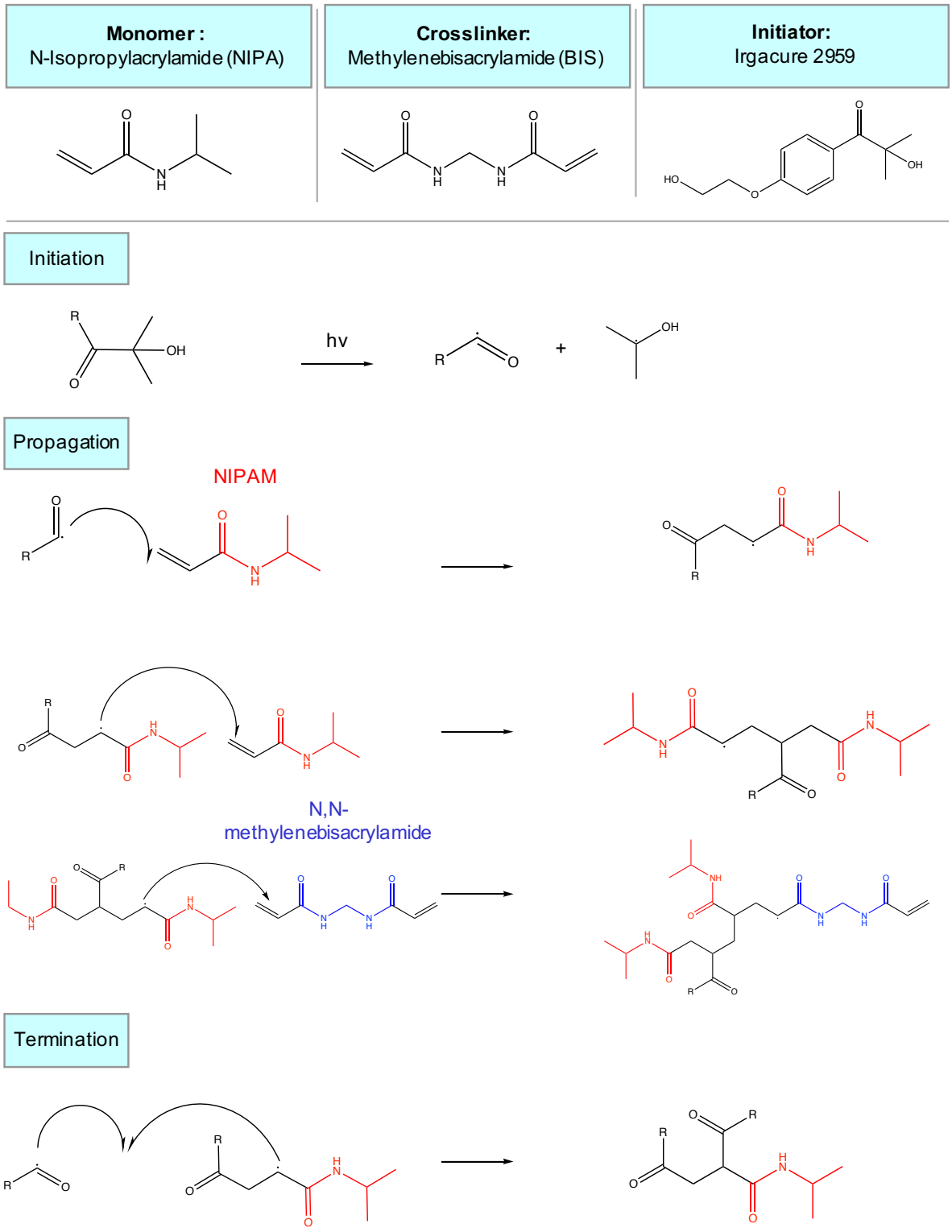

Figure 2.1. Mechanism for free-radical polymerization of a hydrogel.

2.2 Stimuli-Responsive Hydrogels

Stimuli-responsive hydrogels undergo a drastic change in volume in response to an external trigger such as pH, temperature, or solvent composition.[3,4,23,24] N-Isopropylacrylamide (NIPA) is an example of a temperature-responsive monomer (Figure 2.1). The isopropyl group of NIPA gives the monomer and the resulting polymer hydrophobic characteristics. Below 32°C, the isopropyl groups are hydrated by water molecules into a clathrate structure.[25] At temperatures above 32°C, the clathrate structure is disrupted and NIPA chains aggregate due to hydrophobic interactions between the isopropyl groups. This transition is driven by a gain in entropy by the water molecules (hydrophobic effect). As a result, NIPA gels deswell because water is expelled when the NIPA chains collapse. The temperature (~ 32°C) at which this occurs is known as the lower critical solution temperature (LCST). A NIPA gel is transparent below the LCST while the gel appears opaque above the LCST. NIPA has been extensively investigated for applications in drug delivery because of this property.[26] Figure 2.2 illustrates the discontinuity of this transition, i.e. a temperature difference of a few degrees leads to a large change in volume.

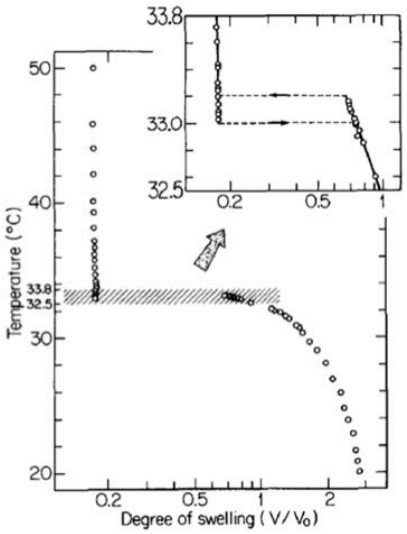

Figure 2.2. Degree of swelling of a NIPA gel in pure water as a function of temperature.[27]

The swelling behavior of hydrogels is also affected by the presence of pendant ionizable groups.[24] For example, the amine groups of 2-(dimethylamino) ethyl methacrylate (DMAEMA) alternate between a neutral and charged state depending on the pH of the solution. If this monomer is used to make a gel, then the gel will respond to pH. The tertiary amine groups are neutral at high pH and therefore the gel will be weakly swollen. However, the amine groups become charged at low pH and electrostatic repulsions between these amine groups leads to an increase in the degree of swelling at low pH.

2.3 Biopolymers

Biopolymers are macromolecules found in nature and can be divided into three main classes: polypeptides, polynucleotides and polysaccharides.[18] For our studies, we will focus on certain polypeptides and polysaccharides, which are discussed in more detail below.

2.3.1 Gelatin

Gelatin is the most abundant animal-derived biopolymer. Gelatin is a protein that is formed by the partial hydrolysis of collagen extracted from the skins and bones of animals such as pigs and fish.[18] Native gelatin forms a gel at room temperature due to the formation of triple helices between Gly-X-Y motifs, where Gly refers to glycine, X is typically proline and Y is typically hydroxyproline. In our experiments in Chapter 4, we modified the lysine residues in gelatin with methacrylate groups to enable photopolymerization. This modification did not affect the formation of triple helices.[28] Most members of a class of enzymes known as matrix metalloproteinases (MMPs) cleave gelatin in its triple helical regions to yield peptide fragments.[29] In our studies, we utilized the MMP, Collagenase Type IV.

2.3.2 Alginate

Sodium alginate is an anionic polysaccharide obtained from brown seaweed. It is widely used for biomedical applications due to its low cost, biocompatibility, low toxicity and the ease of crosslinking. It is a linear unbranched polymer consisting of blocks of 1,4-linked β-D mannuronic acid (M) and α-L guluronic (G) residues (Figure 2.3a).[30] The G-blocks of alginate can interact with specific multivalent ions such as Ca^{2+}, Sr^{2+} or Fe^{3}. These cations form "egg-box" junctions which results in the conversion of an alginate solution into a crosslinked alginate hydrogel (Figure 2.3b). The strength of these alginate hydrogels depends on the ratio of M/G content, the molecular weight and concentration of alginate, and the type of multivalent cation. [31]

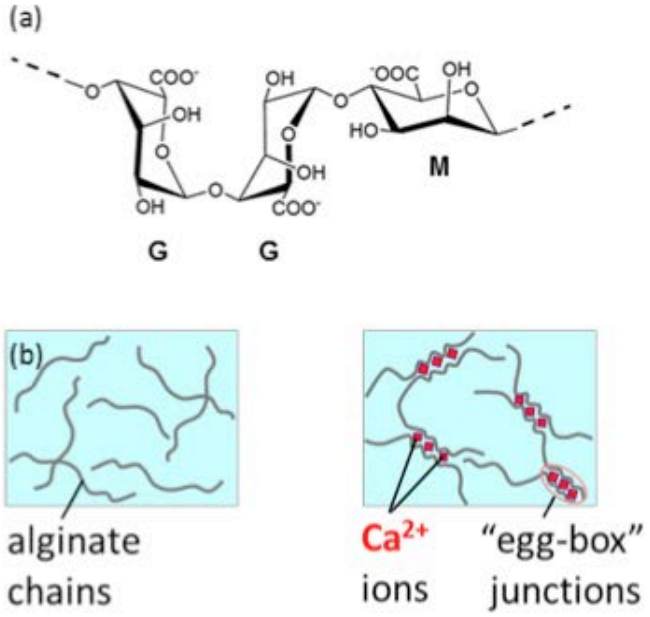

Figure 2.3. (a) The molecular structure of alginate consists of (1-4)-linked β-D-mannuronate (M) and C-5 α-L-guluronate (G) residues. (b) Schematic demonstrating gelation of alginate upon addition of calcium ions. The zones where crosslinking occurs are called "egg-box" junctions.

2.4 Shape-Changing Materials in Nature

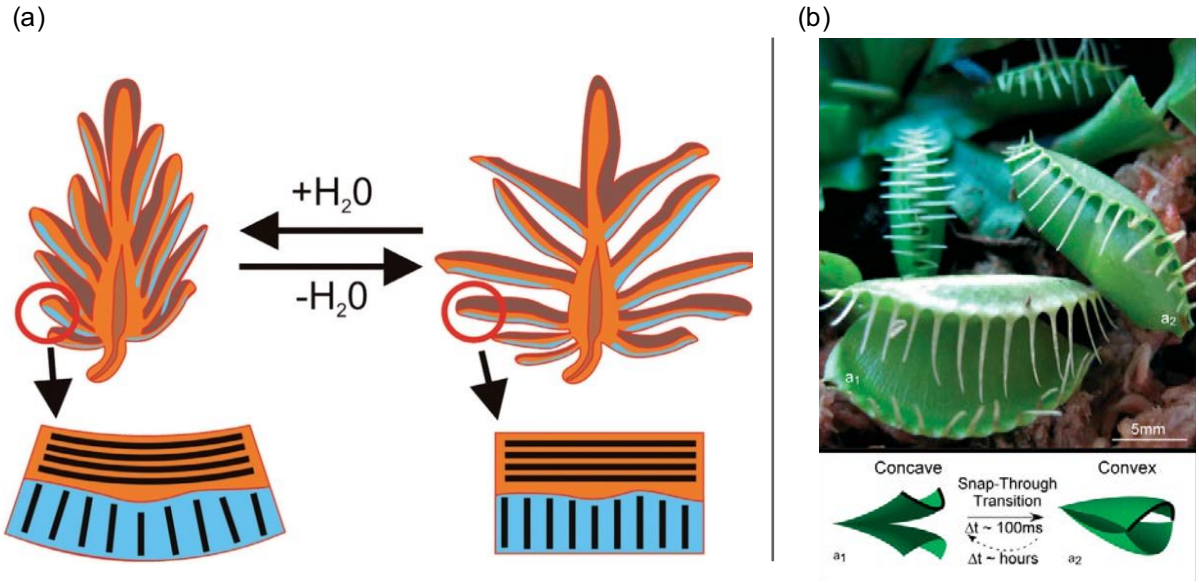

Figure 2.4. (a) Schematic illustrating the actuation of scales in a pine cone in response to changes in ambient humidity.[32] (b) The leaves of the Venus flytrap change from a concave state to a convex state when triggered by an insect landing on it.[33]

The inspiration for the creation of shape-changing soft structures is derived from the morphological changes exhibited by plants in nature. Examples include the closing of mimosa leaves, the opening of pine cones (Figure 2.4a), and the transition of the Venus flytrap from an open to a closed state (Figure 2.4b). These shape changes are driven by changes in swelling (i.e. turgor pressure) between different layers of plant tissue.[11,12] The presence of cellulose fibrils in a swellable matrix lends directionality to the shape transformation. The orientation of the cellulose fibrils dictates the direction of deformation. The matrix preferentially swells in the direction perpendicular to the fibrils. The length of the fibers remains the same. For example, the scales of the pine cone open and close in response to changes in ambient humidity. This movement protects the seeds,

which are only released in drier conditions. Each scale of the pine cone consists of a bilayer structure.[34] As shown in Figure 2.4a, the cellulose fibrils are aligned parallel to the long side of the scale in the upper layer and the fibrils are oriented perpendicularly in the other layer. A decrease in ambient humidity leads to anisotropic contraction and the scales open.

The Venus flytrap (Figure 2.4b) is a carnivorous plant. Its geometry is responsible for its rapid transformation from an open to a closed state.[35] The leaves are double curved when the trap is open. When stimulated, typically by the contact of an insect (prey) in the pocket between the leaves, different regions of the leaf swell, which causes the leaves to change their curvature from concave to convex. As a result, the trap snaps shut, and the insect is trapped for digestion.

2.5 Shape-Changes Induced in Polymer Gels

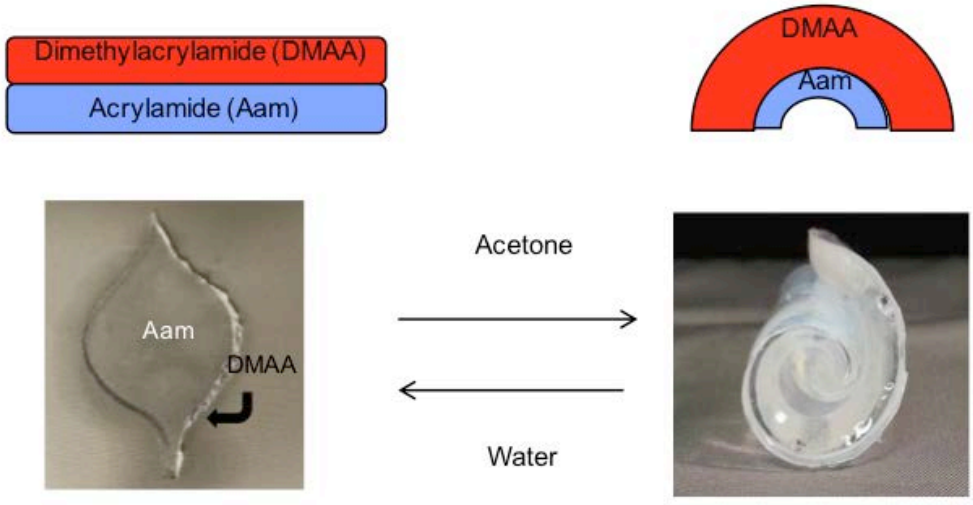

Figure 2.5. Folding of a bilayer gel consisting of two layers: dimethylacrylamide (DMAA) and acrylamide (AAm).

Hu et al. created the first self-folding hydrogel structure. This structure was a "bilayer", i.e., a sandwich of two gels (Figure 2.5), an active layer, acrylamide (AAm) and a passive layer, dimethylacrylamide (DMAA). AAm gels are known to shrink in the presence of acetone. The AAm/DMAA bilayer gel remains flat in water. Note that the AAm and DMAA swell to a similar degree in water. In acetone, the shrinking of AAm causes a mismatch in swelling between the two layers. This induces the flat gel to fold to form a tight scroll. Two criteria must be fulfilled for folding to occur. First, there must be sufficient adhesion between the two layers. If adhesion is poor, the layers will delaminate during differential swelling. Second, the passive layer must be soft and deformable for bending to take place. Overall, bending occurs due to the inhomogeneous expansion or shrinking of a material, which can be induced by a change in external conditions (such as temperature, pH, or solvent quality). The shape of the 2D planar film determines the resultant 3D shape. For example, rectangular bilayer gels form tubes. In comparison, star-shaped films form flower-like structures.

The folding of hydrogels is analogous to the bending of a bimetallic strip consisting of two metals with different thermal expansion coefficients. In both cases, certain regions of the structure expand more, which causes the whole structure to bend and fold. Hydrogels undergo significantly larger changes in volume compared to the thermal expansion of metals. This thermal expansion of metals has been utilized for over a century in thermal switches. The general theory regarding bilayer bending was discussed by Timoshenko in 1925.[36] He modeled a bimetallic strip and assumed that it can only bend in one direction.

$$\frac{1}{\rho} = \frac{6(\varepsilon_2 - \varepsilon_1)(1+m)^2}{h(3(1+m)^2 + (1+mn)\left(m^2 + \frac{1}{mn}\right)} \tag{2.1}$$

$$\frac{E_1}{E_2} = n \tag{2.2}$$

$$\frac{a_1}{a_2} = m \tag{2.3}$$

where E_1 and E_2 are the elastic moduli of each layer, a_1 and a_2 are the thicknesses of each layer, h is the total thickness (a_1 + a_2), ε is the actuation strain, and ρ is the radius of curvature. The subscripts 1 and 2 correspond to layer 1 and 2 respectively. This equation does not predict the direction of folding and is only applicable for elastic deformations in one direction.

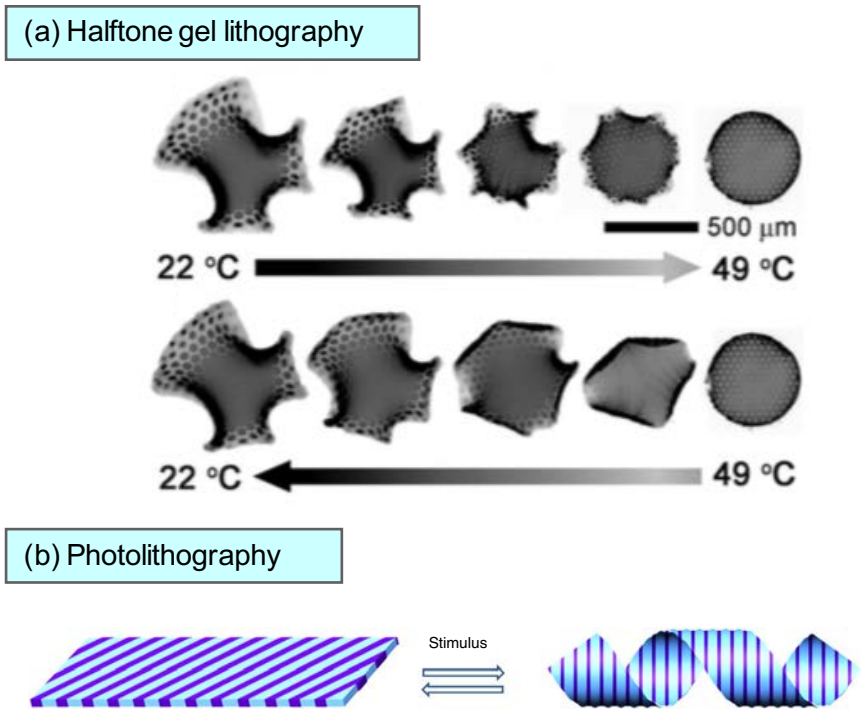

Figure 2.6. Examples of 3D structures created by patterning gels with regions of differential crosslinking. (a) 3D structures are created due to differential swelling between the highly crosslinked dots in a low crosslinked matrix.[37] (b) Photopatterning was utilized to create alternating strips of different chemical composition and thereby

degrees of swelling. The flat sheet formed a helical structure in response to an external stimulus.[38]

Techniques such as photolithography, molding, and electron-beam lithography have been utilized to fabricate hydrogels with swelling heterogeneities. One technique known as "halftone" photolithography is where the gel precursor is exposed to different extents of UV light.[37] This technique yields a gel with regions of different crosslinking densities and therefore different degrees of swelling, as shown in Figure 2.6a (the dark grey dots are more crosslinked than the light grey matrix). Regions of lower crosslinking will swell more. As a result, the flat sheet transforms into an Enneper's surface at 22°C while it flattens out at 40°C. Similarly, Wu et al. utilized photolithographic techniques to create alternating stripes of two different gels within the same sheet (Figure 2.6b). The two gels have different swelling responses in water as a function of temperature. As a result, upon heating, the flat sheet transformed into a helical tape.[38]

There are many examples of hydrogel structures that respond to triggers such pH, temperature and solvent. However, there are few examples of structures that respond to unconventional stimuli such as biomolecules or applied electric fields. Smela et al. utilized an electric field to trigger the folding of a patterned gold film with polypyrole hinges. The first example of an enzyme-sensitive structure was demonstrated by Gracias et al. The structure consisted of a pre-stressed metallic structure with biopolymer hinges. In the presence of the specific enzyme, the hinge is degraded and the structure folds. Our lab has also fabricated polymeric hydrogel structures that respond to the presence of specific biomolecules. This work is described in further detail in Chapter 3.

Chapter 3

Enzyme-Triggered Folding of Hydrogels

The results presented in this chapter have been accepted for publication in the following journal article: J. C. Athas, C. P. Nguyen, B. C Zarket, A. Gargava, Z. H. Nie and S.R. Raghavan, "Enzyme-Triggered Folding of Hydrogels: Toward a Mimic of the Venus Flytrap", *ACS Applied Materials and Interfaces*, in press (2016).

3.1 Introduction

Polymer hydrogels, made by the polymerization of monomers and crosslinkers, constitute a widely studied class of soft materials.[3,4,39,40] Such gels are three-dimensional networks of polymer chains connected at junction points by covalent bonds (crosslinks). When placed in water, these gels swell to a volume that is much larger than their dry volume.[41] A striking feature of many gels is that their volume sharply changes in response to external stimuli such as temperature or pH.[39,40] Such volume changes can be discontinuous (step-like) and reversible. For example, gels of N-isopropylacrylamide (NIPA) remain swollen at low temperatures up to 32°C, but shrink at temperatures above 32°C. Thus, NIPA gels show a discontinuous response to temperature at 32°C, which is the lower critical solution temperature (LCST) of NIPA.[39,40] In addition to changes in gel volume, which occur isotropically in the entire material, gels can also be made to undergo specific changes in their *shape*.[11,12,42,43] For example, flat gel sheets have been induced to transform into open helices or closed helical tubes in response to temperature, pH, or light.[7-9,11,12,38,42-45]

One motivation to study hydrogels is the existence of many soft gel-like materials in nature.[11,42] These include creatures that live in water such as squids and jellyfish as well as land animals such as worms. Additionally, the natural inspiration for shape-changing gels comes from plants. The prototypical example of a plant that changes shape is the Venus fly trap,[35,46-50] an insectivorous plant with two large leaves that form a cup or wedge shape (see photos later). When an insect lands on the inner portion of the cup, the two leaves fold inward, trapping the insect, which is thereafter digested by the plant. Other examples of shape-changing plant-based materials include wheat awns and seed pods.[1,2] The driving force for shape changes in plants often comes from the differences in swelling ratio (i.e., turgor pressure) between adjacent types of plant tissue. Thus, it is important to recognize that soft materials in nature are not homogeneous; on the contrary, they can have many different zones with distinct chemical and mechanical properties. In creating biomimetic responsive gels, one should therefore look to mix and match different kinds of gels within a single hybrid material. Recently, several techniques have emerged to create such hybrid gels including soft lithography,[8] ionoprinting[51] and a method introduced by our lab to create three-dimensional (3D) hybrids by polymerization of viscous monomers[52].

In this chapter, we report the synthesis of hybrid gels that change shape in response to specific biomolecules (enzymes) at low concentrations. The shape changes we demonstrate include the folding of a flat gel sheet into a closed helical tube and the transition of a Venus flytrap analog from an open to a closed state. While several studies have explored the use of biomolecules as triggers for gels,[19,53,54] most of these studies

have been conducted in the context of molecularly-imprinted gels, where the binding of biomolecules merely induces the gel to swell or shrink. To our knowledge, the only biomolecule-triggered *shape* change reported in small objects was in the work of Gracias *et al*.,[15] which was on a complex material made by electron-beam lithography that contained both metallic portions as well as a hinge made from a polymer gel.

Biomolecular binding or enzymatic reactions have many unique features: for one thing, they are highly specific, i.e., they occur in a lock-key fashion between enzyme-substrate or biomolecule-ligand.[55] Also, very low (micro- to nanomolar) concentrations of biomolecules are adequate to induce substantial responses at the cellular level.[19,55] Thus, the challenge in our study was not only to drive a large macroscopic change in gel shape using biomolecules, but to do so using minuscule concentrations of these molecules in solution. To achieve this, we have designed a A/B/C hybrid gel, as described below, where A, B, and C correspond to distinct chemistries, and only one of the three undergoes an enzymatic reaction. The enzyme-induced change, in turn, creates differential stresses in the gel sheet, which ultimately causes the sheet to change shape.[56] We believe such shape-changing gels will be of interest to researchers working in a variety of areas, including in soft robotics, in the design of biomimetic materials, and in the creation of biosensing platforms and biomedical implants. As one example, we show that the shape-changing property of these gels could serve as a macroscopic signal for the presence of certain physiologically relevant enzymes.

3.2 Materials and Methods

Materials. The monomers PEGDA (535 Da), PEGDMA (330 Da), and NIPA, and the reagents methacrylic anhydride (94%), octadecyl-trichlorosilane (OTS) (≥ 90%) and toluene were purchased from Sigma Aldrich. Copper (II) sulfate (anhydrous powder), gelatin from porcine skin (gel strength 300, Type A) and EDTA (ACS reagent) were also purchased from Sigma Aldrich. Ethanol was from Pharmco-Aaper while the UV initiator Irgacure 2959 was from BASF. The inorganic clay laponite-XLG was obtained from Southern Clay Products. Phosphate buffered saline buffer was also purchased from Sigma Aldrich. The collagenase type IV enzyme (305 U/g) was from Worthington Biochemical Corp. NIPA was recrystallized using hexane as a solvent to remove any inhibitor. All other chemicals were used as received. Ultrapure deionized water from a Millipore system was used for all experiments.

Synthesis and Characterization of Gelatin Methacrylate (GelMA). GelMA was prepared using the procedure described by Nichol et al.[57] Briefly, 10% (w/v) gelatin was dissolved in PBS by heating to 65°C. 5% (v/v) methacrylic anhydride was then added and the temperature was maintained at 65°C for 2 h. Afterwards, the solution was diluted with 5X PBS to stop the reaction. The solution was dialyzed against DI water using a membrane with a 12-14 kDa cutoff at 40°C for a week. The purified solution was then lyophilized and the dry powder was stored in a freezer. To verify attachment of methacrylate groups to gelatin, ^{1}H-NMR spectra were collected on GelMA in deuterium oxide at 65°C using a Bruker AVANCE 600 Hz spectrometer.

Preparation of Hybrid Gels. All monomers were dissolved in DI water through which nitrogen gas had been bubbled for 30 min to remove dissolved oxygen. In each case, 0.5 % (w/v) of Irgacure 2959 was added as the UV initiator. For Gel A, the pre-gel solution contained 20 wt% of PEGDA. For Gel B, the pre-gel solution was composed of 10 wt% of lyophilized GelMA and 5 wt% of PEGDMA. For Gel C, 1 M of NIPA was first dissolved and then 3.5 wt% of laponite was slowly added to the solution while stirring to avoid clumping.

Glass slides (75 mm × 25 mm) coated with OTS were used in preparing gels. The OTS coating ensures that the gels can be easily detached following UV polymerization. For this, slides were rinsed with ethanol and then immersed in a solution of 0.2% OTS in toluene for 15 min. The slides were then rinsed several times with toluene to remove excess OTS, then dried by placing in an oven at 90°C for 1 h.

A reaction cell was made using two glass slides separated by double-sided tape on two ends. The Gel A precursor solution was introduced into the cell and UV polymerized through a photomask (Figure 3.2a). All photomasks were designed on Adobe Illustrator CS6 and printed on transparencies using a Brother Multifunction Laser Printer. The UV light source was a Xenon RC500 lamp which emitted radiation over the entire UV spectrum. Following polymerization, unreacted monomer was rinsed off the reaction cell using DI water. Then the Gel B precursor was introduced (Figure 3.2b) and polymerized. Next, another layer of double-sided tape was added to adjust the height of the reaction cell. Finally, Gel C precursor was introduced into the cell and polymerized by UV light

(Figure 3.2d). The hybrid gel was then peeled off the reaction cell, and cut to the dimensions shown in Figure 3.2e. Gels were soaked in DI water overnight to remove unreacted monomer. For preparing the other gel designs such as the Venus flytrap analog, the same procedure was used, but with different photomasks.

Rheological Studies. Dynamic rheological experiments were performed on a AR200 stress-controlled rheometer (TA Instruments). Experiments were done at 25°C using 20-mm parallel plates on gel disks of diameter 20 mm and thickness 1 mm. A solvent trap was used to minimize drying of the samples. Frequency sweeps were conducted within the linear viscoelastic regime of the sample, determined separately from strain-sweep experiments.

Swelling Measurements. Disks of Gels A, B, and C, were separately made with a diameter of 20 mm and a thickness of 1 mm. The disks were immersed in DI water and allowed to swell for 24 h. Next, the disks were blotted dry using a Kimwipe and weighed. Afterwards, the disks were lyophilized and weighed again. The swelling ratio Q was calculated as the ratio between the swollen and dry weights.

Cell Culture and Cell Lysate. Mouse fibroblast cells (L929) were purchased from ATCC, as was Eagle's modified essential medium (EMEM). Penicillin-streptomycin (Pen-Strep), Fetal Bovine Serum (FBS) and trypsin were purchased from Gibco. For L929 cell culture, EMEM was supplemented with 10% FBS and 1% Pen-Strep. The cells were cultured in T-75 flasks in a 37°C incubator with 5% CO_2. Cells were passaged

approximately twice a week and media was exchanged every two days. To obtain cell lysate, the cultured cells were typsinized and resuspended in PBS at a concentration of 10^6 cells/mL. The solution was then sonicated on ice for a total time of 1 min at a power of 180 W (10 s of sonication followed by 10 s of rest). Following sonication, the clear lysate left behind was used in further studies.

3.3 Results and Discussion

3.3.1 Fabrication of Hybrid Gel Sheets

The hybrid gels designed here contain three different crosslinked polymers, designated as A, B, and C in Figure 3.2. These polymers are confined to specific zones in the overall hybrid. The hybrid has two thin layers, each about 75 μm thick, that are sandwiched together to form a "bilayer". The bottom layer has gels A and B arranged in alternating strips. The top layer is composed only of gel C. Each of these polymers was chosen based on different considerations. Gel A is based on polyethylene glycol diacrylate (PEGDA), which is a monomer with two crosslinkable acrylate groups. Gels of PEGDA are relatively stiff and do not swell much. Gel B is a copolymer of gelatin methacrylate (GelMA) and polyethylene glycol dimethacrylate (PEGDMA). The GelMA is the one material in our study that is sensitive to biomolecules. It is obtained by attaching methacrylate groups to the backbone of gelatin using a method reported in the literature.[57,58] Figure 3.1 shows the reaction scheme as well as evidence from ^{1}H-NMR for the modification. From the spectra, the degree of methacrylation in the GelMA used here is estimated to be about 60%. The GelMA is crosslinked together with PEGDMA (two methacrylate groups) to form Gel B. Finally, Gel C is based on N-

isopropylacrylamide (NIPA). To crosslink NIPA, rather than use a bifunctional monomer like bis-acrylamide (BIS), we use nanoparticles of a synthetic clay called laponite (these are disks with a diameter of 25 nm and a thickness of 0.9 nm).[52,59] Laponite (LAP) disks serve as crosslinking junctions, i.e. the polymer chains extend from one face of a disk to another.[59] The reason for using laponite is that the resulting gels are more flexible than those formed with bifunctional monomers.[45,52]

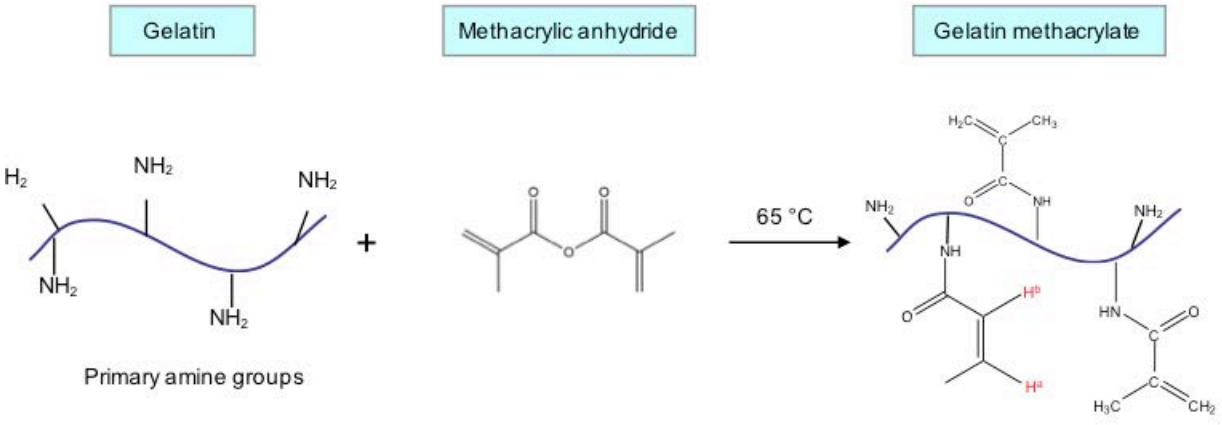

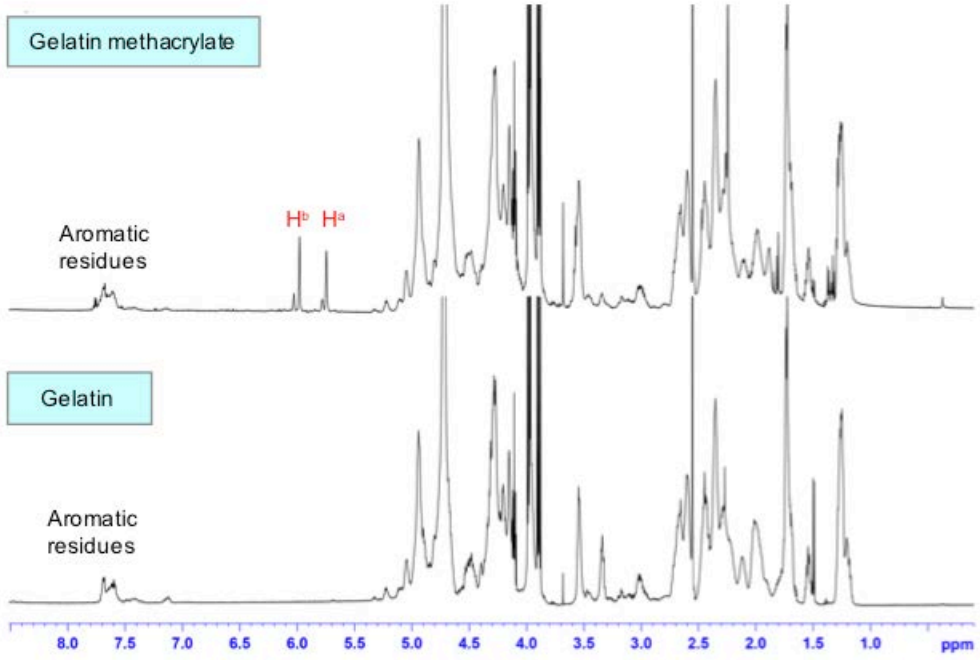

Figure 3.1. Synthesis of gelatin methacrylate and analysis by ^{1}H NMR. The reaction scheme is shown on the top.[57] Lysine and arginine residues in gelatin are converted to methacrylate groups by reaction with methacrylic anhydride. NMR spectra are compared for the parent and synthesized polymer. The peaks H^{a} and H^{b} at 5.6 ppm confirm the addition of methacrylate groups to gelatin. The integrated intensities due to the aromatic residues, H^{a} and H^{b} were used to estimate the degree of functionalization (i.e., the ratio of the number of amino groups modified with methacrylate to the initial number of amino groups.[58] Here, the degree of functionalization is about 60%.

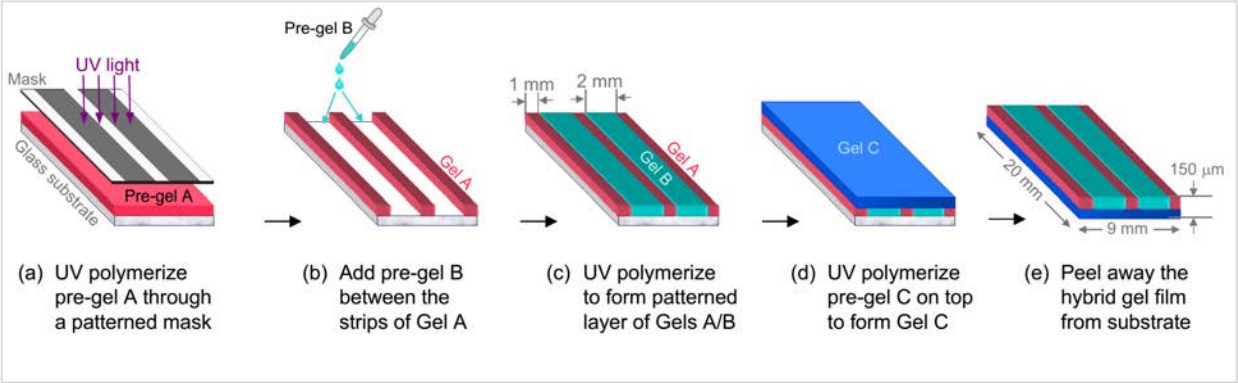

Figure 3.2. Synthesis of hybrid gels having three components by UV-photolithography. Gel A is PEGDA, Gel B is a copolymer of GelMA and PEGDMA, and Gel C is NIPA crosslinked with laponite nanoparticles. The various steps to form the hybrid gel are indicated in (a) to (e) on the figure. The final gel shown in (e) is a thin, rectangular film with the dimensions indicated, and it is a sandwich of two layers. The top layer has alternating strips of Gel A and Gel B, while the bottom layer is Gel C.

We utilized UV-photolithography to fabricate our hybrid gel sheets (Figure 3.2). A home-made photomask consisting of alternating black (2 mm wide) and clear (1 mm wide) strips was printed on transparencies. Ultraviolet (UV) light passes through the clear areas whereas it cannot penetrate the black ones. First, we spread a pre-gel solution of Gel A (i.e., 25 wt% PEGDA and initiator) between two glass slides and exposed it to UV light through the photomask (Figure 3.2a). The solution was gelled in the areas

corresponding to the clear sections of the mask while the adjacent areas remained liquid. The ungelled liquid was washed off and then the pre-gel solution of Gel B was poured such that it filled the areas between the Gel A strips (Figure 3.2b). The Gel B precursor solution contained 10 wt% GelMA, 5 wt% PEGDMA and initiator. Upon UV irradiation, Gel B strips were formed between the Gel A strips (Figure 3.2c). Lastly, the spacer height was increased and the precursor solution to Gel C (15 wt% NIPA, 3.5 wt% laponite, and initiator) was introduced above the A/B layer, and this was crosslinked by UV light to form the Gel C layer (Figure 3.2d). The final gel could be peeled away from the glass substrate and it had dimensions of 20 mm × 9 mm × 0.15 mm.

3.3.2 Spontaneous Folding of Gels in Response to Enzyme

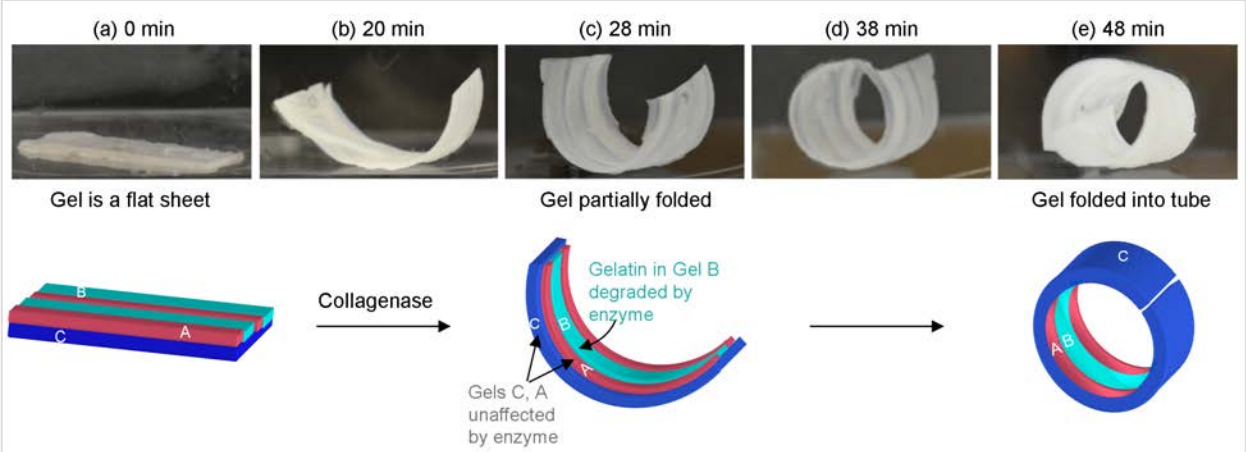

Figure 3.3. Folding of a hybrid-gel sheet upon exposure to collagenase enzyme. At t = 0, 50 U/mL of collagenase is added to the solution. Initially, the gel is flat, but with time it folds into a closed tube, as shown in photos (a) to (e) that correspond to representative time points. The effect of the enzyme is to degrade the gelatin in Gel B, thereby softening the A/B layer. This causes the C layer to fold over the A/B layer, as shown by the schematics.

We first studied the hybrid gel sheets in different media. The sheets remained flat in water, regardless of pH or salt concentration. They also remained flat in organic solvents such as ethanol or acetone. We then proceeded to study the effect of adding the enzyme collagenase to the aqueous solution surrounding a gel sheet. Collagenase is an enzyme from the class of matrix metalloproteinases (MMPs) that degrades certain portions of a gelatin gel into peptide fragments (note that gelatin is denatured collagen).[60] Specifically, collagenase looks for triple-helical segments where three individual gelatin/collagen chains bind together (native gelatin forms a gel at room temperature due to such physical junctions[61]). Although we have modified gelatin with methacrylates to make GelMA, this does not affect the chains' ability to form triple-helical junctions.[57,58] Thus collagenase can still act on the GelMA chains in the Gel B portion of the sheet.

Figure 3.3 shows the response of a gel sheet to 50 units/mL of collagenase (type IV), which is introduced into the solution at $t = 0$. Over a period of 45 min, the flat sheet spontaneously curls up to form a closed tube of radius ~ 2 mm. The curling of the sheet is driven by the enzymatic degradation of GelMA, which causes the Gel B regions of the sheet to lose crosslinks and hence become weaker. The mechanism for this shape change is discussed below. Note that the folding of the sheet occurs out-of-plane about an axis perpendicular to the length of the Gel A strips, as illustrated in Figures 3.3b-e. This is observed regardless of the aspect ratio of the sheet. The reason, as will be discussed below, is that the Gel A strips are relatively stiff. Therefore, folding along the axis perpendicular to the Gel A strips is more favorable than other alternatives.

We now quantify the kinetics of the shape change (flat sheet to folded tube) shown in Figure 3.4 using image analysis software. Specifically, when the gel is partially folded, we draw a circle that overlaps onto the bent gel (i.e., the gel forms an arc of this circle), as shown in Figure 3.4. This is termed the "equivalent circle", and the radius of this circle becomes smaller as the gel continues to bend and fold. Eventually, the gel is folded into a closed tube, i.e., there is no gap between the gel ends (Photo 2). At this point, the equivalent circle coincides with the tube cross-section and the radius of this circle approaches 2 mm. Given further time, the tube continues to fold inwards, i.e.., the two ends start to overlap, but the radius of the tube does not decrease much. Even after 24 h in the enzyme solution, the tube remains folded at roughly the same radius.

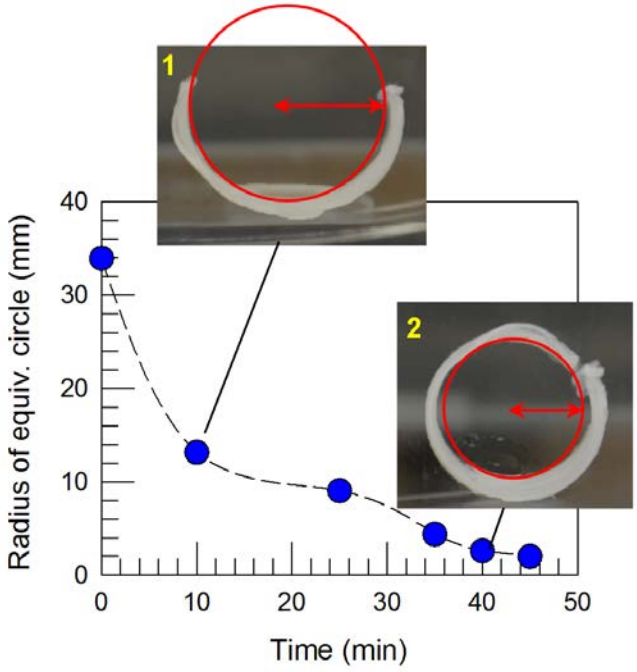

Figure 3.4. Kinetics of gel folding from flat sheet to tube. The folding shown in Figure 3.3 in response to 50 U/mL of collagenase is quantified by image analysis. At each time point, the image of the gel (side view) is mapped to an "equivalent circle", as shown in Photos 1 and 2. The radius of this circle quantifies the extent of folding. As shown in the plot, this radius decreases with time, ultimately plateauing at the radius of the closed tube.

As a first step to proving that gel folding is indeed caused by the enzyme, we study the effect of enzyme concentration. An enzyme unit (U) is defined as the amount of enzyme that catalyzes the conversion of 1 micromole of substrate per minute. Here, we varied the concentration of the collagenase (type IV) enzyme from 60 U/mL to 0.75 U/mL. In each case, we used identical gel sheets and measured the time taken for a flat sheet to curl to form a closed tube (with a radius ~ 2 mm). As noted above, this "response time" was 45 min from Figures 3.3 and 3.4 for the case of collagenase at 50 U/mL. A plot of the response time vs. enzyme concentration is shown in Figure 3.5. We see a roughly linear drop in response time as enzyme is increased in the range between 10 to 60 U/mL. This suggests a direct correlation between response time and reaction kinetics: i.e., the expected linear increase in reaction rates with enzyme concentration[55] is consistent with a linear decrease in response time. Below 10 U/mL, however, the response time increases in a nonlinear fashion as the enzyme content is decreased. This deviation from the linear trend may be because other factors, such as the mass transfer rates for enzyme into the gel, begin to play a role. In any case, it is worth noting that very low amounts of enzyme (< 1 U/mL) are still able to induce the folding of the gel. Also, since the enzymatic degradation is irreversible, the enzyme-induced transition from a flat to folded gel is a one-time process.

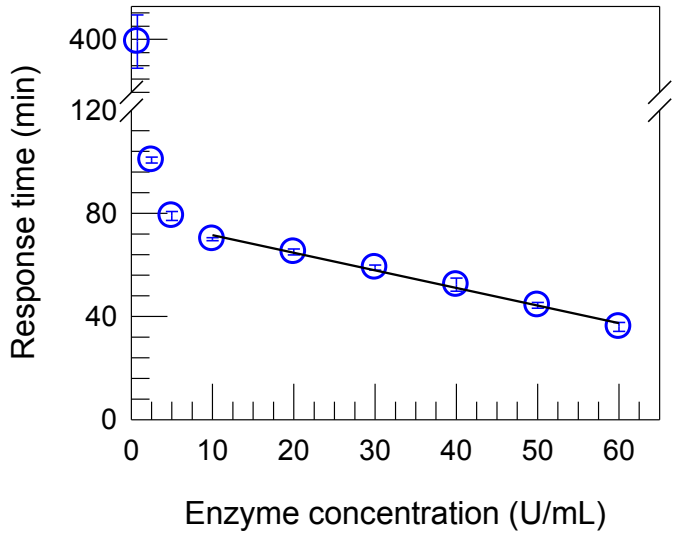

Figure 3.5. Effect of enzyme concentration on gel folding. The response time is defined as the time taken for a gel sheet to transform into a closed tube with a radius ~ 2 mm. The plot shows that this time decreases monotonically with enzyme concentration. A linear decrease is observed between 10 to 60 U/mL of enzyme. The error bars represent the standard deviation from 3 measurements.

3.3.3 Mechanism for Gel Folding

To better understand folding, we studied the mechanical and swelling properties of the three gels A, B, and C in the hybrid, both in the absence and presence of enzyme. For this, we made disks of each gel, 20 mm in diameter and 1 mm in thickness. These were studied under oscillatory shear in a rheometer and the elastic G' and viscous G'' moduli were measured as a function of frequency. As expected, all gels showed an elastic response, with the moduli being independent of frequency and $G' > G''$.[62] Thus, we can characterize each gel by its gel modulus, i.e., its value of G'. We find (Figure 3.6) that Gel A (PEGDA) is stiff (G' = 20,300 Pa), whereas Gel C (NIPA-LAP) is relatively weak (G' = 1,850 Pa). Both these gels are unaffected by the presence of collagenase. Gel B (GelMA-co-PEGDMA) is also weak at the start (G' = 1,450 Pa). and moreover, its

modulus decreases in the presence of collagenase. The plot in Figure 3.6 shows that, upon contact with 50 U/mL of enzyme, the G' of Gel B drops from 1,450 to 750 Pa over the first 30 min and subsequently to 200 Pa over a period of 3 h. Over longer periods of time, the Gel B disk loses mass, and after about 6 h there is no trace of the gel in the solution (indicating complete degradation).

Regarding the swelling behavior, we first incubated each of the Gel A, B, and C disks in water in the absence of enzyme for 24 h. The disks were then weighed, then freeze-dried and weighed again. The swelling ratio Q was defined as the mass of the swollen disk divided by the mass of the dried disk. As shown in Figure 3.6, Gels A and B undergo negligble swelling in water ($Q \approx 4.7$ and 6.0, respectively) whereas Gel C swells considerably ($Q \approx 49$). Thus, there is a large swelling mismatch between the bottom (C) and top (A/B) layers of the hybrid gel. This swelling mismatch creates stresses within the film, giving it a propensity to fold, but the high stiffness of the A/B layer prevents folding. Upon incubation with enzyme, Gel B gets degraded, which sharply decreases its modulus (see above) and also causes a modest increase in its swelling ratio (Q increases from 6.0 to 9.1 after 30 min of contact with 50 U/mL of enzyme). Gels A and C remain unaffected by enzyme. Our experiments show that the key effect upon adding enzyme is the decrease in modulus of Gel B, which makes the A/B layer more pliable or compliant. As a result, the stresses created by the mismatch between the swollen C layer and the less swollen A/B layer are relieved when the sheet folds into a tube with the C layer outside and the A/B layer inside.[38,56]

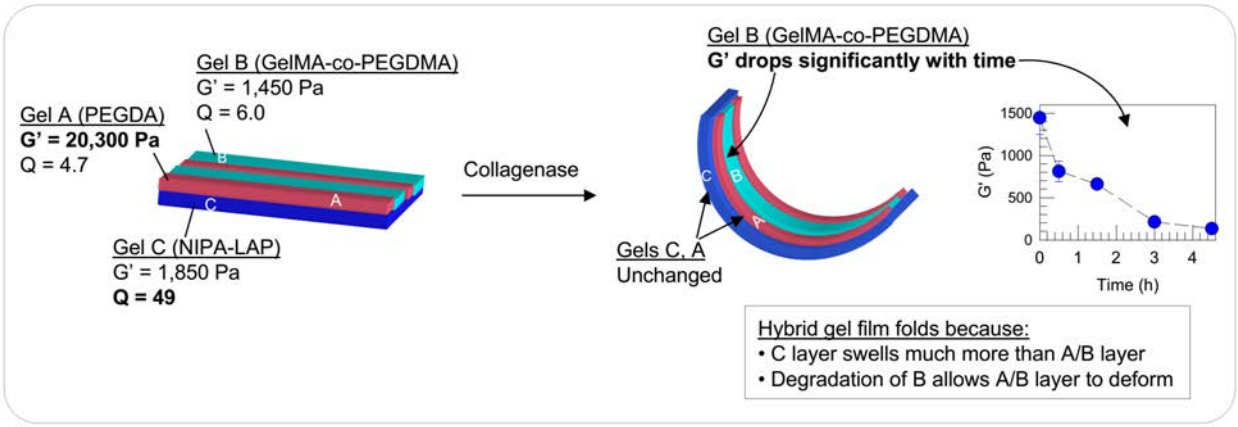

Figure 3.6. Mechanism for enzyme-induced gel folding. Data from two types of measurements are shown for the three individual gels in the hybrid when each of them is placed in water in the absence of enzyme: the elastic modulus *G'* (measure of gel stiffness) and the swelling ratio *Q*. The data reveal that Gel A is much stiffer than the others while Gel C swells much more than the others. The swelling mismatch between the C and A/B layers is the driving force for the folding, but it is opposed by the stiffness of the A/B layer. When exposed to enzyme, Gel B gets degraded, which drops its *G'* as time progresses, as shown by the plot on the right. Thus, the A/B layer becomes softer and more deformable, which allows the C layer to fold over it.

The above reasoning is consistent with theories advanced for the bending of metallic strips as well as for the folding of gel sheets.[36,56] In the case of a metallic strip with a top and a bottom layer, a mismatch in thermal expansion coefficients between the two layers creates stresses when the strip is heated.[36] These stresses can be relieved by bending, provided the strip is not too mechanically rigid. The balance between these two factors is reflected in the Timoshenko equation.[36] For our hydrogel sheets, it is the difference in volume expansion (swelling) of the top and bottom layers that drives the folding. However, folding can occur only if the gel is mechanically compliant. Thus, the concept exploited here is to use an enzyme to turn a stiff layer into a compliant one,

thereby enabling a transition from an unfolded to a folded gel. Support for the above mechanism is also provided by other experiments. For example, we studied an A/C design without Gel B (just two layers of Gel A and Gel C; see Figure 3.7a). In this case, no folding was observed due to the high modulus (G' = 20,300 Pa) of Gel A, which consists of 20 wt% PEGDA. Next, we lowered the concentration of PEGDA used to make Gel A, thereby decreasing the stiffness of the A layer. At 10 wt % PEGDA (G' = 830 Pa), the sheet slightly curled at its ends (Figure 3.7b), but did not fold further. At 5 wt% PEGDA (G' = 320 Pa), however, the sheet folded into a tube (Figure 3.7c). This confirms that folding is prevented by a stiff A layer whereas folding is enabled when the A layer is much more compliant.

Figure 3.7. Folding behavior of bilayers of Gel A (PEGDA) and Gel C (NIPA-LAP). The dimensions of each gel was maintained at 20 mm x 9 mm x 0.15 mm. The NIPA-LAP is identical to that in Figures 3.3 to 3.6. The concentration of PEGDA was decreased from (a) to (c). Note that folding of the flat sheet into a tube is observed only when the PEGDA is reduced to 5 wt%. At higher concentrations of PEGDA, the stiffness of the A layer opposes folding.

3.3.4 Gel Folding in Cell Lysate

We have proven the ability of our hybrid gels to fold in the presence of specific biomolecules. Such a response could have applications in biological contexts; e.g., to signal the occurrence or proliferation of certain diseases. As a first step in evaluating such possibilities, we performed experiments with a class of murine fibroblast cells (L929). Fibroblasts are cells of the connective tissue that synthesize the extracellular matrix (ECM), a major component of which is collagen.[55,63] MMP enzymes that can degrade the collagen in the ECM are expected to be present in these cells (the ECM gets degraded and reformed during normal processes in the body like tissue remodeling as well as during diseased states like arthritis or cancer metastasis).[63,64] We therefore reasoned that the MMPs in L929 cells might plausibly act like the collagenase studied earlier and degrade the gelatin in Gel B. But would the concentration of MMPs in these cells be sufficient to drive folding of our hybrid gel within a reasonable timeframe?

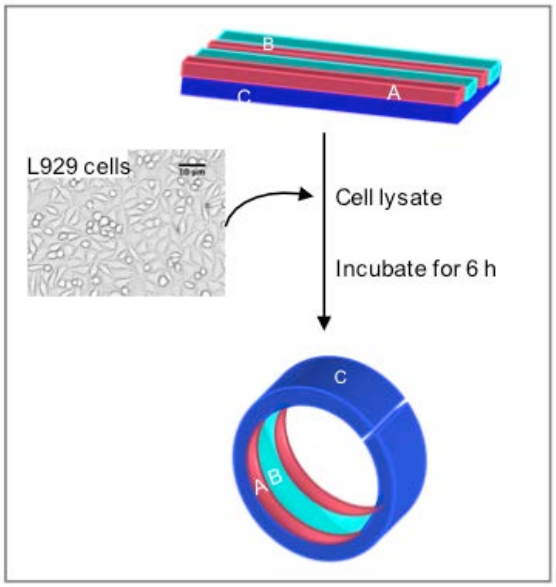

Figure 3.8. Gel folding induced by cell lysate. Mouse fibroblast (L929) cells were cultured and a suspension of the cells was lysed by sonication. This lysate was then introduced into a solution containing the A/B/C gel sheet. The flat gel folded into a tube in 6 h, and the folding is attributed to the presence of MMPs in the lysate (a class of enzymes that can degrade gelatin). The image shows a bright-field optical micrograph of the cells.

To test this, we made a suspension of L929 cells in buffer (10^6 cells/mL) and lysed the cells using a tip sonicator. The resulting lysate was a clear solution, which was then used for further studies. First, we incubated a disk of Gel B alone in the cell lysate. This gel degraded completely in a 24 h period, presumably due to breakdown of gelatin by the MMPs. In comparison, disks of Gel A and Gel C remained unaltered. Next, we placed our A/B/C hybrid gel sheet in the cell lysate (Figure 3.8). The gel converted from a flat sheet to a closed tube in about 6 h (photo in Figure 3.9a). To show that the result was due to the action of MMPs, we performed control experiments where we added MMP inhibitors to the cell lysate prior to placing the gel. Two inhibitors, copper sulfate and EDTA, were each tried at a 5 mM concentration. In both cases, the gel did not fold even after 24 h (photo in Figure 3.9b). Additional controls were also done: for example, the gel did not fold in just the cell growth media. Thus, our experiments strongly suggest that the folding is driven by MMPs from the L929 cells and that the typical intracellular (physiological) concentration of MMPs in these cells is sufficient to drive the macroscopic shape-change. From an extrapolation of the response time data in Figure 3.5, we estimate the concentration of MMPs in our lysate to be about 0.1 U/mL (which roughly translates to about 6 nM).

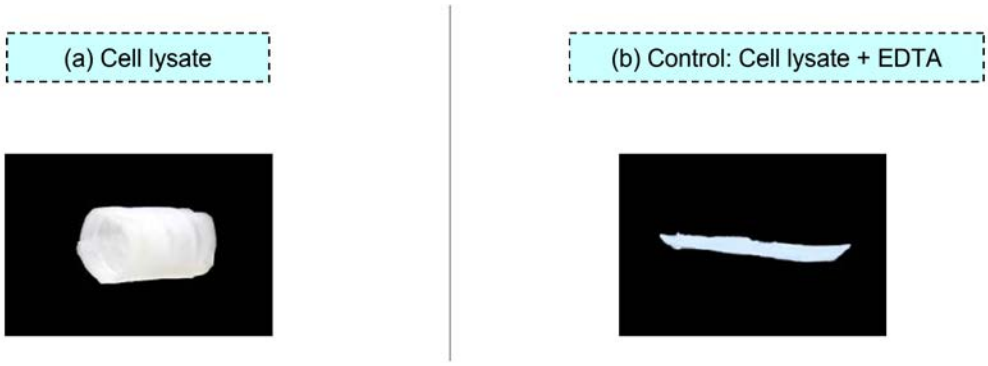

Figure 3.9. **Visual observations of hybrid gels folding in cell lysate.** Mouse fibroblasts (L929) cells were cultured and the cell lysate was obtained. The hybrid gels were then incubated in the cell lysate. (a) The initial flat sheet folded to form a tube in 6 h due to the presence of MMPs in the lysate. (b) As a control, we added 5 mM EDTA (an inhibitor of MMPs) to the lysate. In this medium, the gel sheet remained flat.

3.3.5 Venus Flytrap Analog

While the folding of a single gel is interesting on its own, we can also incorporate a folding gel into other inert structures and thereby engineer other shape transitions. As an example, we have created an analog of the Venus fly trap based on hydrogels (Figure 3.10). Photos 1-3 show an actual Venus fly trap in action. As noted in the Introduction, the two adjacent leaves of the plant form a wedge-shaped compartment (Photo 1). The leaves have hairs that are sensitive to touch, and so when an insect settles into the compartment and touches the hairs, the two leaves move together (Photo 2) and completely close (Photo 3), thereby entrapping the insect. The precise mechanism is believed to involve induction of differential turgor pressure in the upper and lower portions of the leaves.[35,46-50] The leaves bend, and in the process store elastic energy. A sudden release of this elastic energy explains why the trap can close rapidly (in about 0.3 s).

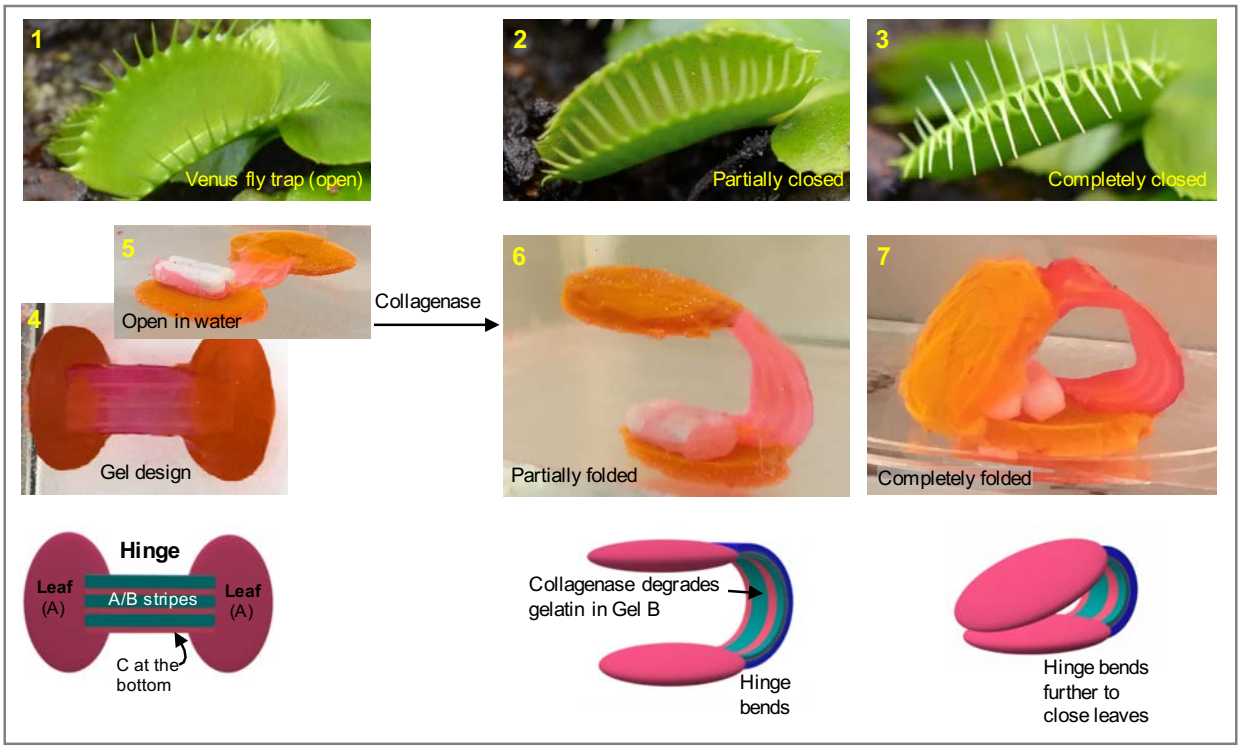

Figure 3.10. Hybrid gel that mimics the behavior of a Venus flytrap. Photos 1-3 show a Venus flytrap plant, which has a wedge-shaped cavity flanked by two leaves. When an insect falls in the cavity, the leaves close thereby capturing the insect for subsequent digestion. Photo 4 shows the design of our gel-based Venus fly-trap mimic, and this is schematically shown below the photo. The rectangular hybrid gel from Figure 1 is affixed as a hinge to two flat panels ("leaves") made of Gel A. The hinge has dimensions of 20 mm x 9 mm x 0.15 mm while each leaf is a disc with dimensions of 20 mm x 15 mm x 1 mm (thus the leaves are much thicker than the hinge). Photo 5 shows that the structure is flat in water. A load (two magnetic stir bars) is placed on one of the leaves. When exposed to collagenase, the hinge bends, and thus the leaves close around the load, as shown in Photos 6 and 7. The schematics show the directionality of bending: in the hinge, the C layer is outward while the A/B layer is inward.

Our mimic of the Venus flytrap is shown in Photo 4 and is illustrated schematically below the photo. Two oval "leaves" made of Gel A (PEGDA) are connected by a "hinge" or "stem" made from our usual hybrid gel (A/B strips on top, C on the bottom). The leaves are chosen to be rigid structures unaffected by enzyme, while the hinge is designed to fold on exposure to enzyme. The entire

structure was created by photocrosslinking and it remains a flat sheet in water. A load is placed on one leaf (Photo 5). When collagenase is added to the water, it removes crosslinks from Gel B, thereby driving the A/B/C hinge to fold. In turn, the leaf on top folds until it touches the bottom leaf (Photos 6, 7), thereby enclosing the load. The time for the leaves to fold completely is about 50 min for 50 U/mL of enzyme, which is close to the time measured for the folding of a single gel sheet under the same conditions (Figure 3.4). Thus, we have mimicked the shape change of the Venus flytrap, albeit with hydrogels.

3.3.6 Other Shape Changes

Our gel design can be adapted to achieve other transitions in shape upon exposure to enzyme. In some cases, we can predict the final shape *a priori*. An example is the A/B/C design in Figure 3.11a. This design is similar to that in Figure 3.2 but with one difference: the A/B strips in the top layer are at an angle of 45° with respect to the bottom C layer. The overall dimensions are similar to those in Figure 3.2, with the Gel A strips being 1 mm wide and the Gel B strips being 2 mm wide. This gel is initially flat in water and it is then exposed to collagenase. We noted previously that folding occurs along an axis perpendicular to the stiff Gel A strips. Here, because the strips are at an angle, we anticipated that folding would lead to a helix rather than a closed tube. Indeed, the folded structure is seen to be an open, right-handed helix in Figure 3.11a. Similar folding of flat gel strips into helices has been observed in a few studies.[38,45] It is also observed with plant seed pods,[2] and there also the folding occurs perpendicular to the direction of stiff cellulose fibrils that are embedded at an angle within the pods.

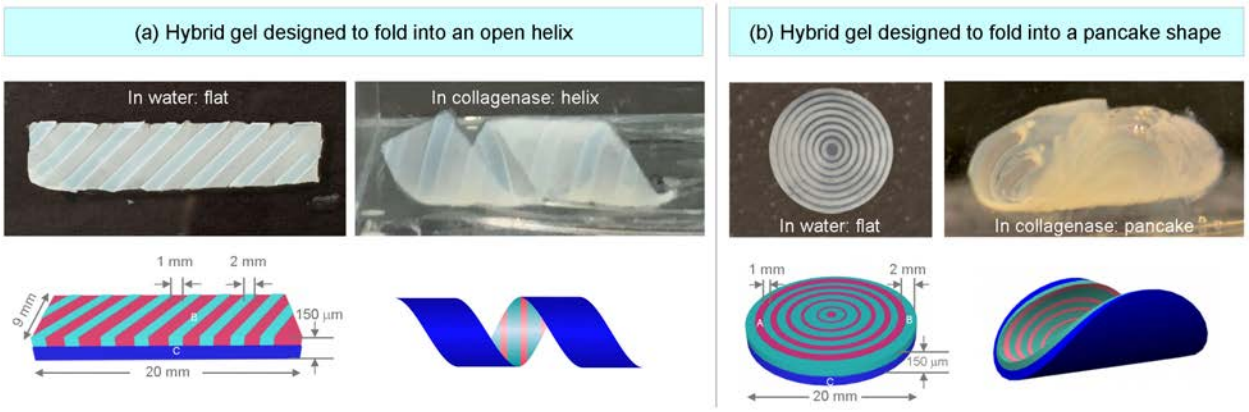

Figure 3.11. Designed hybrid gels that fold into different shapes. Both designs feature three component gels (A, B, and C), as in Figure 1. In each case, photos of the gel in water and in collagenase solution are shown. Schematics of the design and the folded structure are also shown. (a) The design has A/B strips on top at an angle of 45° with respect to the bottom C layer. This gel is a flat sheet in water, but folds into an open, right-handed helix when exposed to collagenase. (b) A design with concentric circles of A and B in the top layer and C in the bottom layer. In this case, the gel folds into a pancake shape in the presence of collagenase.

A second design of a folding gel is shown in Figure 3.11b. This is an A/B/C design in the form of a disc rather than a rectangular sheet. As before, the bottom layer is Gel C while the top layer has alternating concentric circles of Gels A and B. The Gel A circles are 1 mm thick while the Gel B circles are 2 mm thick. In this concentric design, there is no preferred axis for the gel to fold. Instead, when the flat gel is placed in collagenase solution, it transforms into the shape of a folded pancake (Figure 3.11b). The swollen Gel C layer is on the bottom while the A/B layer is on the top. A gel patterned with a series of concentric circles was recently studied by Kumacheva *et al*.,[44] and in that case the folded shape was similar, but with negative curvature in the middle, i.e., resembling a saddle rather than a pancake. More detailed analysis of the above geometry is beyond the scope of the present paper. In closing, we reiterate the versatility of our

system, which permits a variety of shape changes to be induced by enzyme with the same underlying materials, but with different designs.

3.4 Conclusions

We have designed gels that undergo a transformation in shape when exposed to low concentrations of a specific enzyme. The typical transformation is from a flat sheet to a folded tube. Our motivation in creating these gels was to expand the range of triggers for gel systems beyond the common ones like temperature and pH. Moreover, our approach to accomplishing these objectives focused on physical, rather than chemical design, i.e., without resorting to extensive synthetic chemistry.

Towards this goal, we have put forward a design for "hybrid" gels, involving three individual gels with distinct properties. Gel C swells highly in water compared to Gels A and B, while Gel A is much stiffer than the rest. Gel B is the one that is sensitive to enzymes. All gels are based on common, commercially available monomers, with the exception of Gel B, for which we synthesized a methacrylated version of gelatin. We integrated the three gels together into thin-films using UV polymerization through homemade photomasks. The base design involves an A/B layer on top of a C layer. When placed in water, the sheet is initially flat despite the swelling mismatch between the layers. When collagenase enzyme is added, it cleaves the gelatin chains in Gel B, thus reducing the stiffness of the A/B layer. This allows the swollen C layer to fold over the A/B layer. The time to fold can be tuned by the concentration of enzyme.

The versatility of our underlying A/B/C design is shown by modifying the physical pattern to achieve other shape changes. For example, we can engineer the folding of flat sheets into helices or saddle shapes, instead of tubes. We have also constructed a structure reminiscent of the Venus flytrap. This structure transforms from an open to closed state upon exposure to enzyme, with the "leaves" on either end trapping objects in the middle. In summary, our study highlights the possibility of creating complex designs using hydrogels that could more closely mimic structures seen in nature, both in terms of their form as well as their function. Hybrid hydrogels such as the ones demonstrated here could have potential applications in tissue engineering, soft robotics and biosensing.

Chapter 4

Glucose-Triggered Folding of Hydrogels

4.1 Introduction

In Chapter 3, we described hydrogel films that folded into tubes or other shapes under the action of an enzyme. One drawback of this system is that, because the enzyme cleaves the polymer chains in one of the components of the hydrogel, the folding is not reversible. That is, a folded tube cannot be converted back to a flat film and made to fold again. As an alternative, it would be useful to devise a folding scheme for hydrogels that can occur repeatedly and reversibly. This is the focus in the current chapter. We still retain the focus on enzyme-triggered folding, but now we embed the enzyme in one of the layers of a hybrid gel. Thereafter, we explore whether folding can be induced by the substrate for the enzyme. As noted before, enzymatic reactions are highly specific. The reaction will not occur even if there are small changes in the molecular structure of the substrate. This means that enzymatic reactions can be used to distinguish between very similar molecules, e.g., stereoisomers of a given moiety.

The key enzyme we use in this study is glucose oxidase (GOx), and its corresponding substrate is glucose. GOx catalyzes the conversion of glucose to gluconic acid and hydrogen peroxide (H_2O_2).[65] It is cheap, readily available and stable at high temperatures and over a range of pH values.[66] The product of the enzymatic reaction is H_2O_2, which is a strong oxidizer and an electroactive species.[67,68] Thus, GOx is widely used for the electrochemical detection of glucose, which is the common mechanism in

many commercial glucose meters.[67,68] Such meters are commercially available for use at home by diabetes patients to monitor their glucose levels in blood or urine.[67,68] There is also a need for detecting levels of glucose (and other sugars) in beverages made with sugar or sugar-substitutes. In addition to electrochemical detection methods, there also exist glucose sensors that rely on visual observation, e.g., test strips or dipsticks that change color when exposed to glucose.[69] One advantage of these visual methods is that glucose measurements can be done without the need for a power source to power the device. However, colorimetric detection requires distinguishing between similar colors, which can make it unreliable and difficult to interpret.

Researchers have also attempted to induce easily-observable macroscopic changes in a system upon exposure to glucose. One example is hydrogels that respond to glucose by undergoing a change in volume (shrinking or swelling).[54,70] In this case, the volume change needs to be substantial to be detectable visually. Another approach developed in our lab has been to induce the gelation of a biopolymer, such as sodium alginate upon addition of glucose.[71] In this case, the macroscopic change was the glucose-induced conversion of a sol (thin solution) of alginate to a gel that held its weight in an inverted vial (the difference could thus be revealed by simply inverting the sample vial). The mechanism for gelation again relied on GOx and its reaction product, gluconic acid. The acid solubilized particles of calcium carbonate and thus generated Ca^{2+} ions, which crosslinked alginate chains into a gel.

Our approach in the current study is in a similar vein to the above approaches in that we target a glucose-induced macroscopic response, viz., the folding of a flat rectangular gel into a tube. In effect, the enzymatic catalysis of glucose using GOx is amplified and transduced into a shape-change of the gel. For this, we create a gel that has two thin layers sandwiched together to form a "bilayer". One layer is passive and it contains two enzymes: GOx and catalase. Catalase is used because it increases the efficiency of GOx by degrading H_2O_2.[72] For the active layer, we use a gel based on an amine-containing monomer. At ambient pH, the amines in the gel are uncharged, whereas at lower pH, the amines become charged, causing this layer to swell. The overall mechanism is that the enzymatic reaction on glucose lowers the pH (due to production of gluconic acid) and thus induces a swelling mismatch between the layers of the gel. In turn, the gel sheet folds into a tube.

The above shape change occurs only in the presence of glucose and the kinetics of folding depends on the glucose concentration. For this reason, the shape change can be used as an indicator of glucose in solution. Furthermore, this shape transformation is reversible, i.e. the tube unfolds back to a flat sheet when placed in water and it refolds again when fresh glucose is added. Thus, the gels are reversible and reusable. In addition to the simple bilayer, we can also combine the active and passive layers in other patterns within an overall gel, so as to engineer transitions from flat gel sheets to shapes other than tubes. Overall, our approach yields a low-cost, portable sensor for glucose that can be used without the need for specialized instrumentation. We demonstrate here its use to discriminate between beverages that contain glucose and those that do not. In addition to

sensors, these gels could also conceivably be used to create self-regulating valves or other devices that transition from an open state when no glucose is present to a closed state when the glucose concentration exceeds certain levels.

4.2 Experimental Section

Materials. The following chemicals were purchased from Sigma Aldrich: the monomers 2-hydroxyethyl methacrylate (HEMA) and 2-(dimethylamino)ethyl methacrylate (DMAEMA); the crosslinker Ethylene glycol dimethacrylate (EGDMA); the enzymes GOx (from Aspergillus Niger; Type VII, lyophilized powder ≥ 100,000 U/g) and catalase (lyophilized powder, 2000-5000 U/mg); and fructose. D-Glucose was obtained from Gibco and methyl red from TCI. Corn syrup was purchased from the local grocery store. Citric acid from Carolina Biological and sodium phosphate, dibasic from J. T. Baker were used to make buffer solutions. The photoinitiator Irgacure 2959 was obtained from BASF. Ultrapure water from a Millipore system was used for all experiments.

Preparation of Hybrid Gels. All monomer solutions were dissolved in ultrapure water, which had been degassed for 30 min to remove any dissolved oxygen. HEMA was prepared in two steps. First, mixture A was prepared by mixing 64 wt% HEMA, 0.68 mol% of EGDMA (with respect to HEMA) and 0.5 wt% Irgacure 2959. GOx and catalase were dissolved at the desired concentrations in ultrapure water. This solution was then added to mixture A. For HEMA-co-DMAEMA, the pre-gel solution contained 53 wt% HEMA, 10.6 wt% DMAEMA, 0.68 mol % of EGDMA (with respect to HEMA) and 0.5 wt% Irgacure 2959.

The reaction cell consisted of a glass slide and a plastic slide separated by double-sided tape on the ends. The use of a plastic slide allows the reaction cell to be disassembled easily. HEMA containing GOx and catalase was introduced into the

reaction cell. The reaction cell was then exposed to UV light. The UV source was a Spectroline Long Wave Ultraviolet Lamp 365 nm (Spectronics Corporation). After polymerization, the reaction cell was disassembled. Another layer of double-sided tape was used to increase the height of the spacer. HEMA-co-DMAEMA was then introduced and polymerized. The gels were cut to the dimensions of 25 mm by 9 mm. For preparing various 3D structures, photomasks were designed using Adobe Illustrator CS6 and printed on transparencies using a laser printer.

Rheological studies. Dynamic rheological studies were conducted on disks of hydrogels that were 20 mm wide and 1 mm thick. Experiments were conducted at 25 °C using 20-mm parallel plates. A solvent trap was utilized to minimize drying of samples. Frequency sweeps were conducted within the linear viscoelastic regime of the sample, determined separately from strain-sweep experiments.

Swelling measurements. Disks of HEMA and HEMA-co-DMAEMA that were 20 mm wide and 1 mm thick were fabricated. The gels were allowed to swell in ultrapure water for 24 h. The disks were then blotted dry with a Kimwipe and weighed. Afterwards, the gels were lyophilized and reweighed. The swelling ratio Q was calculated as the ratio between the swollen and dry weights.

4.3 Results and Discussion

4.3.1 Fabrication of Hybrid Gels

The hybrid gels utilized in this study consisted of a bilayer of two polymers A and B. The synthesis of this bilayer gel is illustrated in Figure 4.1. The two layers were selected where one layer would swell in response to changes in pH, while the other layer would remain unaffected. The bottom layer is Gel A, which is HEMA crosslinked by EGDMA, and this layer contains the enzymes GOx and catalase. The upper layer is Gel B, which is a copolymer of HEMA and DMAEMA, again crosslinked by EGDMA. DMAEMA is the active component in our gel and it was chosen because it is pH-sensitive, i.e., its pendant amine groups are expected to become ionized at pH below 4.[24,73] Each layer of the hybrid gel was made to be 75 mm thick. Thus, the overall gels are rectangular strips with dimensions of 20 mm × 9 mm × 150 mm.

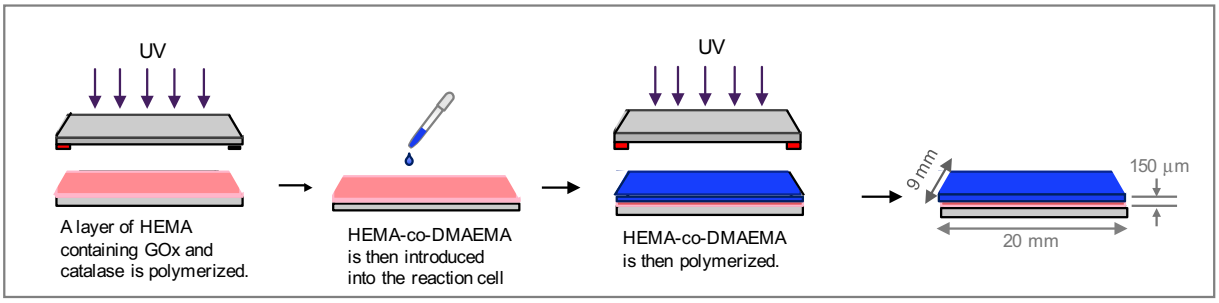

Figure 4.1. Fabrication of hybrid gels. Gel A is HEMA containing GOx and catalase. Gel B consists of HEMA-co-DMAEMA. The different steps associated with fabrication are indicated.

4.3.2 Glucose-Induced Folding of Gels

Figure 4.2 illustrates the enzymatic reactions involving GOx and catalase. GOx catalyzes the conversion of dissolved glucose to gluconic acid and H_2O_2. Catalase is

frequently used in tandem with GOx because it serves two purposes. First, it decomposes H_2O_2 (a by-product of the GOx reaction) into O_2, which is required for the GOx catalysis.[74] Second, if the H_2O_2 was left in the solution, it could reduce the activity of GOx.[72,75] Thus, the incorporation of catalase overcomes issues with GOx and allows both reactions to proceed smoothly.

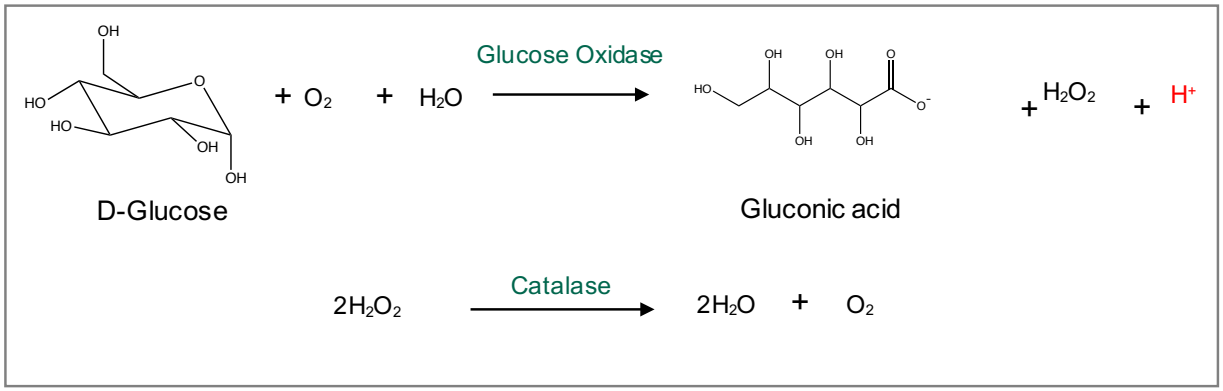

Figure 4.2. Enzymatic reactions involving GOx and catalase.

The folding of A/B bilayer gels in glucose solutions was then systematically studied. For our experiments, the enzyme concentrations in Gel A were chosen to be 500 U/mL of GOx and 125 U/mL of catalase. (Previous studies have shown catalase at about 1/4th the level of the GOx maximizes their synergy.)[76,77] Initially, the gels are flat in both water at ambient pH and in phosphate-buffered saline (PBS). Time-lapse images of the gel in a 0.4 M glucose solution are shown in Figure 4.3. As time progresses, the gel sheet is seen to fold out-of-plane into a closed tube. Note that folding occurs about the short axis of the rectangular side, which is similar to the observations for the gels in Chapter 3. The two ends of the strip come into contact at the 16 min mark, forming a tube with an inner radius of ~ 3.5 mm. After this time, the gel continues to fold and the two ends

overlap to form a tight scroll, as shown in the photo at 45 min (the inner radius is reduced to 2.5 mm in this case). With further time, the radius of the tube remains unchanged at this lower value.

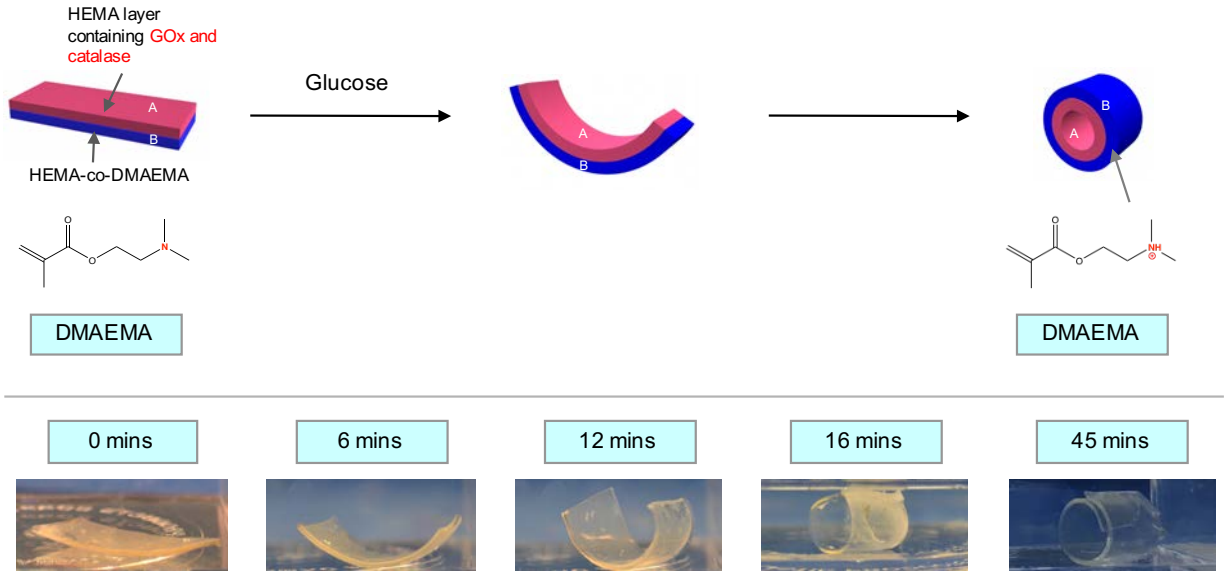

Figure 4.3. Folding of a gel sheet in glucose solution. The solution contains 0.4 M glucose and the gel contains 500 U/mL of GOx and 125 U/mL of catalase. The gel is initially flat. As time progresses, the gel starts folding about its short side, as indicated by the schematics. GOx converts glucose to gluconic acid. As a result, the amine groups in DMAEMA become protonated (indicated in the structure), causing Gel B to swell. This creates a swelling mismatch with Gel A, which causes the B layer to fold over the A layer.

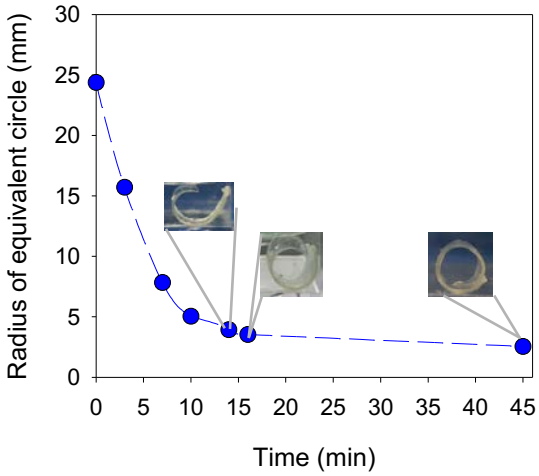

Figure 4.4. Kinetics of gel folding. The data correspond to the images in Figure 4.3 and are for a gel in 0.4 M glucose. At each time point, three points were selected on the curved gel and used to draw a circle, the radius of which is plotted. Side images at selected points are also shown.

We used ImageJ and a three-point ROI plugin to analyze the time-lapse images.[78] Three points were selected on each curved gel and used to draw a circle. Figure 4.4 provides the data for the folding seen in Figure 4.3, i.e., in a 0.4 M glucose solution. As expected, the radius of the circle decreases with time and saturates at long times. Next, we examined the folding of these gels as a function of glucose concentration. In all cases, the same dimensions were maintained (20 mm × 9 mm × 150 mm) as well as the same enzyme concentrations in Gel A (500 U/mL GOx and 125 U/mL catalase). The response time is defined as the time for a flat sheet to form a tube with an inner diameter of ~ 3.5 mm, i.e., when the ends just touch. Figure 4.5 demonstrates that the response time decreases monotonically with increasing glucose concentration. The highest glucose concentration tested was 0.5 M and in this case, the response time was ~ 10 min. This is a relatively quick response and it is about 4× faster than the response to external enzyme in Chapter 3. In addition to substrate, the enzyme concentration is the other variable that affects the response time. We found that reducing the GOx to 50 U/mL (and proportionately reducing the catalase) increased the response time by about 15-fold.

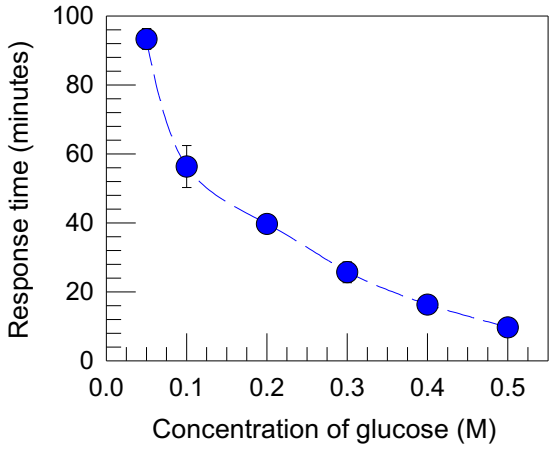

Figure 4.5. Effect of glucose concentration on gel folding. The response time is defined as the time taken for a flat sheet to form a tube with an inner radius ~ 3.5 mm. Increasing the substrate concentration leads to a decrease in response time. The error bars represent the standard deviations from 3 measurements.

Several additional points about these glucose-sensitive gels are worth discussing. First, note that the substrate (glucose) is expected to diffuse into the gel and react with the enzyme. Also, the products of the enzymatic reaction, such as gluconic acid, are expected to diffuse out into the water and change the local pH. This pH change is crucial to the mechanism behind the folding (see below). While these small molecules can diffuse in and out of the gel, we expect the enzyme to remain entrapped in the gel, and be unable to diffuse out. Is this a reasonable assumption? To test this, we incubated a gel containing GOx and catalase in water for 6 h. We then removed an aliquot of water and analyzed it using UV-Vis spectroscopy for the presence of enzyme. No enzyme could be detected, which corroborates our assumption.

A related aspect is the mesh size of the gel. We have deliberately chosen a very high concentration of monomers in both gels. In Gel A, which contains the enzymes,

there is 64 wt% of HEMA, which is expected to lead to a very dense polymer network. One way to estimate the mesh size of Gel A is from rheological measurements. The dynamic rheology of Gel A shows a typical gel-like response with frequency-independent elastic (G') and viscous (G'') moduli. The value of G' is the gel modulus G, which is related to the mesh size x of the gel by:

$$G = \frac{k_B T}{\xi^3} \tag{4.1}$$

where k_B is the Boltzmann constant and T is the absolute temperature.[79] For Gel A, G = 210 kPa, giving a mesh size ~ 2.7 nm. This is smaller than the size of globular proteins like GOx and catalase, which have molecular weights of 160 kDa and 250 kDa, respectively, and are thus expected to have diameters ~ 10 nm.[80] Hence, the enzymes should remain entrapped in the gel.

Another important aspect is the reversibility of the shape transition. When the folded gel is removed from the glucose solution and returned to water at ambient pH, the gel unfolds and reverts to its initial flat state. This behavior strongly suggests that the initial folding was induced by pH, as discussed below. When glucose is then added to the aqueous solution, the gel folds again. Thus, the folding behavior is repeatable multiple times and is observed even days after the gel was prepared. There is no observable increase in folding time even after several cycles of folding and unfolding. The only way to account for this repeatability is if the enzymes remain entrapped within the gel. Note that since the enzymes are catalysts, there is no consumption of enzymes due to reaction.

4.3.3 Mechanism for Gel Folding

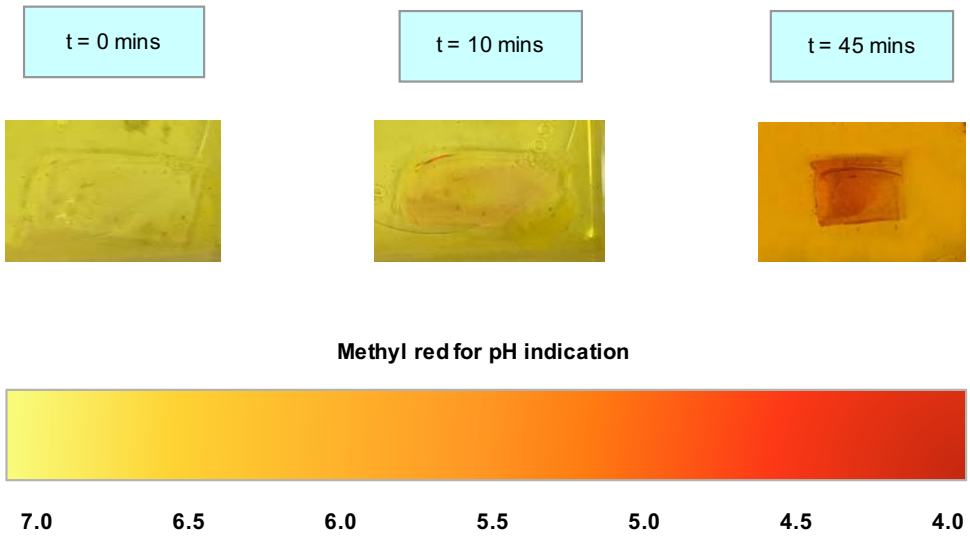

Figure 4.6. Changes in pH during glucose-induced folding of gels. The gel was incubated in a solution containing 0.2 M glucose and methyl red. The gel has an orange tinge at 10 min, indicating a drop in pH, and it is bent into an arc at this point. At 45 min, the gel has a dark orange color, indicating a further drop in pH, and at this point, it is folded. As a reference, the color of methyl red as a function of pH is presented at the bottom.

We now proceed to establish that the folding of the gel is caused by the pH change upon enzymatic reaction. Since the enzymes are present in the gel, any pH change will be local, i.e., initially occur right next to gel. To verify such pH changes, we conducted folding in a solution of methyl red. Methyl red is a pH indicator that turns from yellow to red in acidic conditions, as indicated by the chart in Figure 4.6. At $t = 0$, the glucose solution as well as the gel are yellow. The surface of the gel starts to turn orange as gluconic acid is produced by the enzymatic reaction, and this is clearly evident

at 45 min, by which time the folding of the gel is complete. The color then diffuses through the solution. Note that the color of the gel is darker than the surrounding solution, indicating that the acid (pH drop) originates from the gel. Eventually, the whole solution becomes a dark orange. This experiment confirms that there is a substantial drop in pH at the same time as the gel begins to fold. A further aspect is the morphology of the gel under controlled pH conditions. For this, we prepared citric acid – sodium hydrogen phosphate buffer solutions at various pH and studied identical gels in each solution (in the absence of glucose). Figure 4.7 shows that the gel remains flat at pH 7. However, as the pH is decreased from 6 to 4, the flat sheet folds to form a tube. This occurs because, as the pH is decreased, the amines in Gel B becomes protonated, which makes this layer swell more than the Gel A layer.

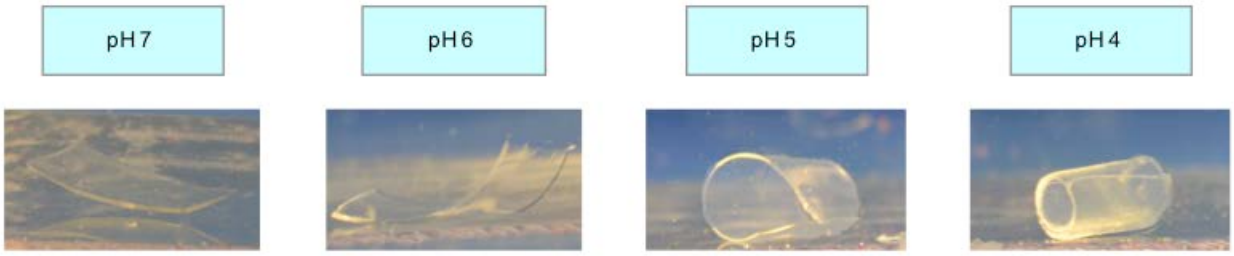

Figure 4.7. pH sensitive behavior of hybrid gels. The gel is flat at neutral pH. However, as the pH is decreased, the amine groups of DMAEMA become protonated. As a result, layer B swells to a greater extent and the gel folds.

Figure 4.8 provides data on the degree of swelling of the two individual gels (A and B) in the above buffer solutions of different pH. The swelling ratios Q of Gel A and Gel B are similar at pH 7. However, when the pH is decreased from 7 to 4, Gel B increases its volume by a factor of 3, whereas the volume of Gel A is invariant to pH.

This difference is expected, and is due to the fact that Gel B transitions from a nonionic gel at pH 7 to an ionic gel (due to the protonation of the amines of DMAEMA) at lower pH. Thus, decreasing the pH leads to a mismatch in degree of swelling between the A and B layers of the gel, which leads to differential stresses at their boundary. These stresses are released when the gel folds from a sheet to a tube. Both gels have comparable and high values of gel modulus ($G' \sim 200$ kPa), and so the folding is not driven (or opposed) by differences in mechanical properties between the layers. Instead, the key factor is the swelling mismatch induced by pH, as indicated in Figure 4.3. Note from the schematics in Figure 4.3 that the more swollen layer (Gel B) forms the outside of the tube while the less swollen Gel A is on the inside of the tube. This is generally the case for gel folding.

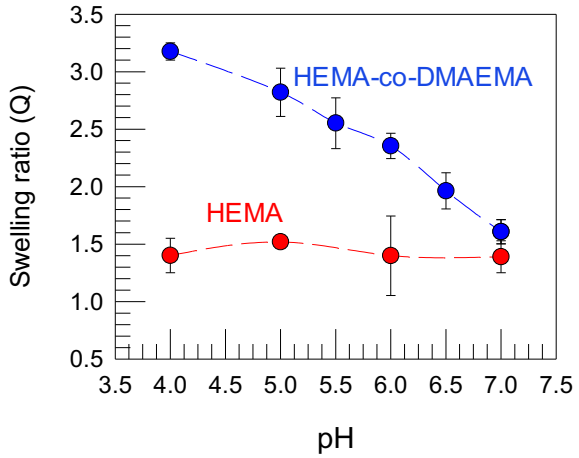

Figure 4.8. Swelling degrees of the two layers in the hybrid gel as a function of pH. The two layers swell to a similar degree at neutral pH. However, as the pH decreases, Gel B swells to a greater extent while Gel A is unaffected by the pH change.

4.3.4 Specificity of Sugars in Inducing Folding

Enzymatic reactions are highly specific.[18] GOx only works on β-D-glucose but not on other sugars. To demonstrate sugar specificity, we tested fructose. No folding was observed in this case. An example is shown in Figure 4.9 for the case of 0.4 M fructose, with the gel remaining flat. Conversely, we tested a commercial product, corn syrup, which is derived from cornstarch and contains glucose. The gel did fold in corn syrup. Thus, the folding of this hybrid gel could be used as a rapid (~ 10 min) and inexpensive test to detect the presence of glucose in an unknown solution. An example is commercial beverages that are sweetened with different sweeteners. This test is insensitive to the color of the sample; however, one limitation is that the pH of the test solution must be close to neutral conditions.

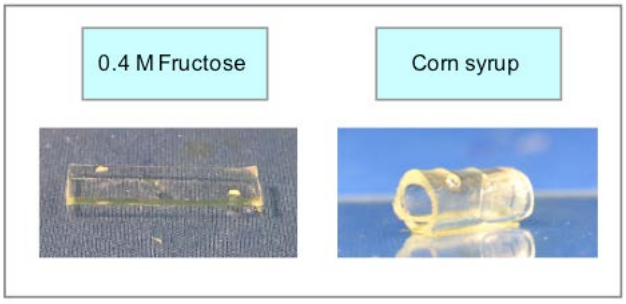

Figure 4.9. Test of folding in the presence of different sugars. The gel remains flat in fructose but folds in solutions containing corn syrup because it contains glucose.

4.3.5 Other structures

We can create different shapes of our initial gels by either cutting out a given shape from a sheet or by using photomasks. The initial shape can be engineered such that the final folded structure assumes a unique 3D shape. For example, in Figure 4.10, we make our initial gel in the shape of a 5-armed star. The gel is still an A/B structure with

the same composition as above, the only difference being that the thickness of each layer was 150 μm (rather than 75 μm in previous studies). The star remains flat in water. However, in the presence of glucose, the arms of the star bend inwards and the overall structure resembles a flower. We found that the thickness of the layers plays an important role in the curvature of the structure. For example, when the thickness of each layer was decreased to 75 μm, the arms of the star folded to form a tubular structure. When the thickness of each of layer was increased to 300 μm, the structure barely folded. These structures can be advantageous since they are striking and can be easily identified by visual inspection.

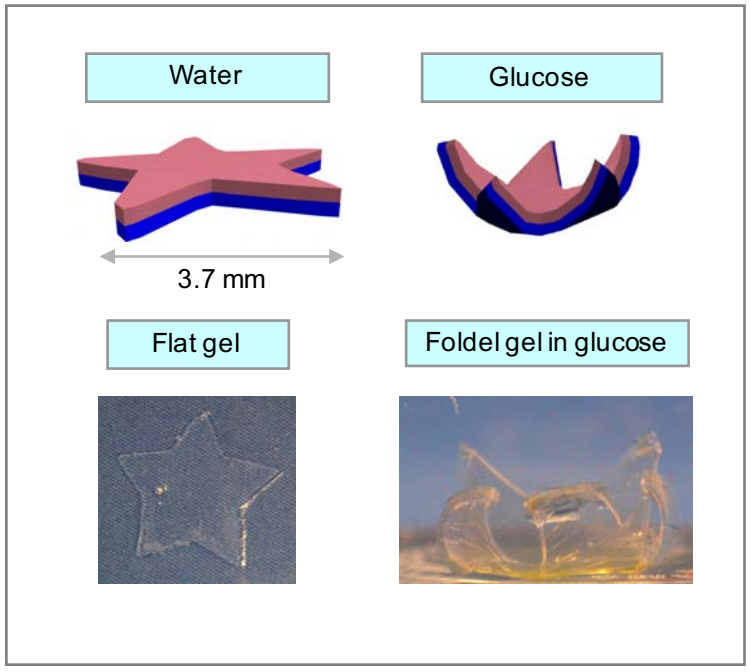

Figure 4.10. Glucose-induced creation of a specific 3D structure. The initial gel was in the shape of a 5-armed star. Initially, the gel is flat in water. In the presence of glucose, the arms bend inwards and the structure resembles a flower.

4.4 Conclusions

We have fabricated bilayer gels that undergo a shape change in the presence of glucose. The gels have two layers A and B, and in layer A, the enzymes GOx and catalase are immobilized. GOx catalyzes the conversion of glucose to gluconic acid. The production of gluconic acid decreases the local pH. The decrease in local pH causes layer B to swell. As a result, the flat A/B sheet folds to form a tube, with a response time of ~ 10 min. The tube unfolds to form a flat sheet when it is transferred to a solution with no glucose present. Therefore, this biomolecule-triggered shape transformation is reversible, meaning the gel is reusable. This shape change only occurs in the presence of glucose and it does not occur in the presence of other small sugars such as fructose. The hydrogels utilized in this study are also biocompatible, which expands their application in areas such as drug delivery or biosensing.

Chapter 5

Multivalent Cation-Triggered Folding of Hydrogels

5.1 Introduction

In Chapters 3 and 4, we studied "bilayer" hydrogels, i.e., those that had two layers sandwiched together to form a planar sheet. In both studies, the bilayer gels transformed from a flat rectangular strip to a folded tube. In both cases, the folding occurred about an axis parallel to the short side of the rectangle, and we classify this type of folding as "short-side folding", as illustrated in Figure 5.1. Most examples of self-folding gels demonstrate this kind of short-side folding.[11] In fact, if the gel is allowed to freely swell in water, short-side folding is always the preferred mode.[20]

The alternative mode of folding occurs about an axis parallel to the long side of the rectangular sheet and can be termed "long-side folding" (Figure 5.1). This has been reported in some rare instances not involving hydrogels, such as in semiconductor membranes.[81] In the case of gels, the only examples of long-side folding are in cases where the gel is constrained prior to folding. For example, gels that were attached to a glass slide had a preference for long-side folding.[82] Alternately, clamping the gel introduces a bias into folding.[83] Once folding is initiated along a certain axis, the gel continues to fold along this axis even when the clamp is removed. Thus, in existing examples of long-side folding, the gels are not allowed to freely swell in water.

Here, we report a new class of self-folding hydrogels that transform from flat sheets to tubes. Our gels are also bilayers, but the structure is new and the stimulus that induces folding is also quite unique. What is most interesting is that in the majority of conditions studied, the gels exhibit long-side folding, resulting in tubes with a narrow diameter. On the basis of experimental observations, we have attempted to provide a hypothesis to account for this unusual folding behavior.

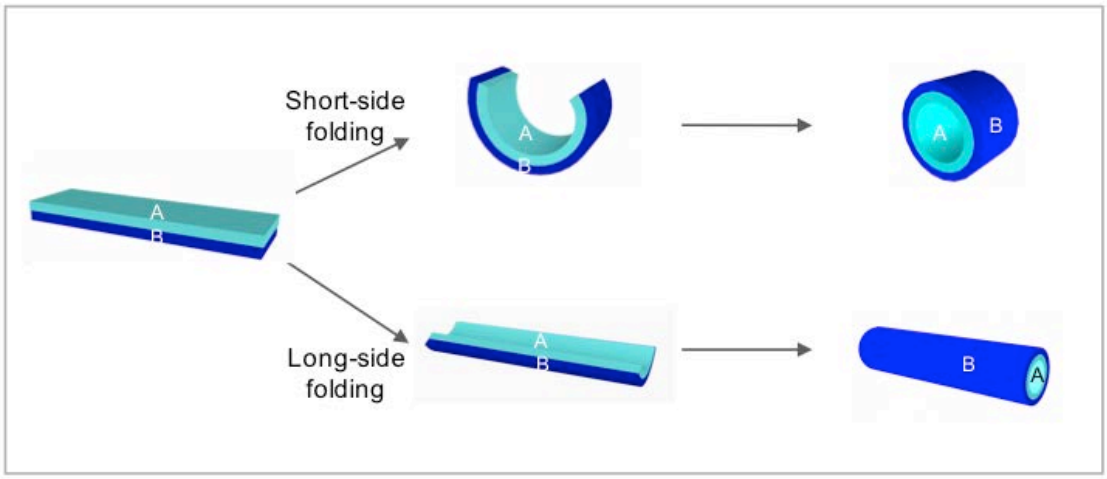

Figure 5.1. Schematic illustrating the two modes of folding: short-side and long-side. The inner diameter of tubes formed by short-side folding are generally larger than that of tubes formed by long-side folding.

5.2 Materials and Methods

Materials. The monomer dimethylacrylamide (DMAA), the crosslinker N,N'-methylene bis(acrylamide) (BIS), and sodium alginate (medium viscosity) were purchased from Sigma-Aldrich. The initiator Irgacure 2959 was obtained from BASF. All materials were used as received. All gels were prepared using ultrapure water. Ethylenediaminetetraacetic acid calcium disodium salt (EDTA), strontium chloride

hexahydrate, calcium chloride dihydrate, iron (III) chloride, copper (II) chloride, and D-(+)-Gluconic acid δ-lactone (GdL) were purchased from Sigma Aldrich.

Hydrogel preparation. All monomer solutions were dissolved in ultrapure water, which had been degassed for 30 min to remove dissolved oxygen. The precursor to Gel A was prepared by mixing 10 wt% DMAA, BIS at a concentration of 1.3 mol% relative to DMAA, the required concentration of alginate, and 0.5 wt% Irgacure 2959 (photoinitiator). The Gel B precursor was prepared by mixing all the above except for the alginate. The hybrid gel was prepared using a reaction cell consisting of two glass slides separated by a spacer. Gel B precursor was first introduced into the reaction cell with two sides of double sided tape used as a spacer. The reaction cell was then exposed to UV light to form Gel B. The reaction cell was then disassembled and the spacer height was increased by using two additional pieces of double-sided tape. Gel A precursor was then introduced into the reaction cell and polymerized to form Gel A. The overall A/B hybrid was then peeled off and placed in the test solution.

Swelling measurements. 1 mm thick gels were created to determine the swelling ratio of the gels. A 20 mm biopsy punch was used to cut out disks from the gel film. The gels were weighed and then were placed in ultrapure water and allowed to swell for 24 h at room temperature. The gels were removed from the water, blotted dry with a Kimwipe and weighed. The extent of swelling was obtained by taking the ratio of the mass of the swollen hydrogel disk to the mass of the initial disk.

Rheological measurements. Rheology was performed on a Rheometrics AR2000 stress-controlled rheometer (TA instruments). Parallel-plate geometry of 20 mm diameter was used with a solvent trap to prevent drying of the sample. Dynamic stress sweep experiments were first performed to identify the linear viscoelastic (LVE) region of the sample. Dynamic frequency sweeps were then conducted in the LVE of the sample.

5.3 Results and Discussion

5.3.1 Cation-Induced Folding

The hybrid gel is an A/B bilayer, with each layer of 150 μm thickness. Gel B consists of DMAA crosslinked with BIS and this is the passive layer. The active layer is Gel A and consists of DMAA-BIS along with the anionic biopolymer, sodium alginate. The alginate is of medium molecular weight (80 to 120 kDa) and is at a concentration of 2 wt%. Alginate chains in Gel A are not crosslinked, but are trapped within the DMAA-BIS network. It is known that alginate undergoes physical crosslinking when multivalent cations such as and Ca^{2+} or Fe^{3+} are added (Figure 5.2). The cations crosslink the alginate chains by forming "egg-box" junctions between the chains.

In our experiments, we start with an A/B bilayer gel that remains a flat sheet in water. When this gel is introduced into an aqueous solution containing one of the above cations at a concentration of 100 to 500 mM, it exhibits long-side folding into a tube (Figure 5.2). Note that the B layer is unaffected by the cations. However, the A layer becomes a double-network gel, i.e., one having two different interpenetrating networks: a chemically crosslinked DMAA network and a physically crosslinked alginate network.[84]

The additional physical crosslinks in Gel A make it stiffer than Gel B, which then causes the A/B bilayer gel to fold. A possible mechanism is discussed later. With respect to the tube, the stiffer A layer is on the inside while the B layer is on the outside. The transition from sheet to such a tube occurs quickly: typically within about 5 min. The inner radius of the tube is generally < 1 mm, which is about 3 times smaller than the tubes formed by short-side folding in Chapters 3 and 4.

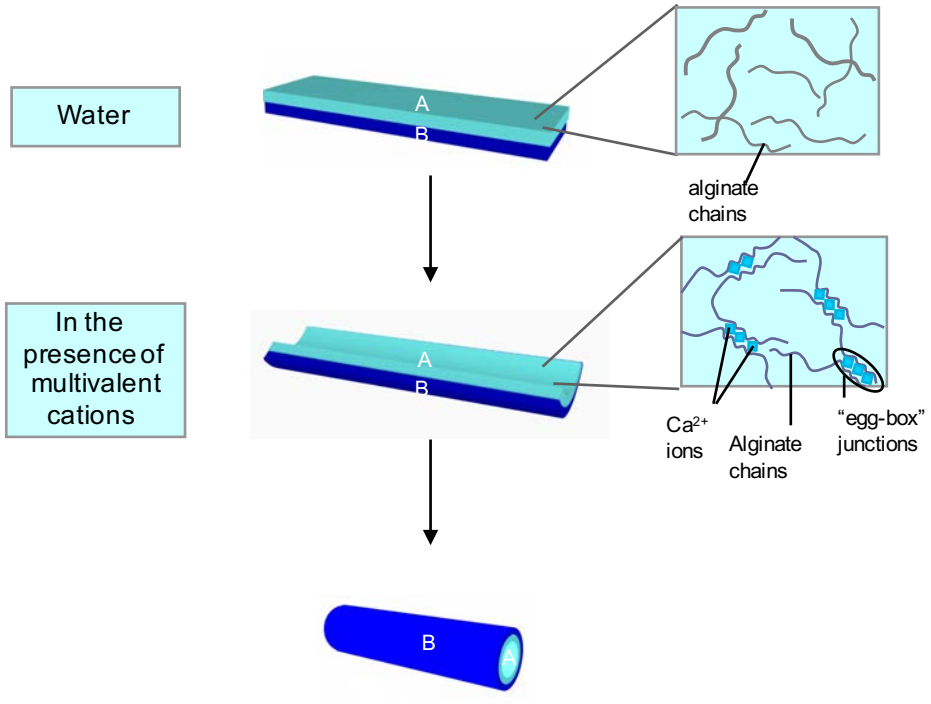

Figure 5.2. Schematic depicting the long-side folding of A/B bilayer gels. Gel B consists of DMAA only, while Gel A consists of DMAA and alginate. Initially, this gel is a flat sheet in water. When multivalent cations like Ca^{2+} are added at a concentration > 100 mM, the alginate in Gel A becomes physically crosslinked into a network that co-exists with the chemical network of DMAA chains. We observe that in such cases, the flat sheet undergoes long-side folding into a tube with Gel B on the outside and Gel A on the inside.

5.3.2 Effect of Cation Type

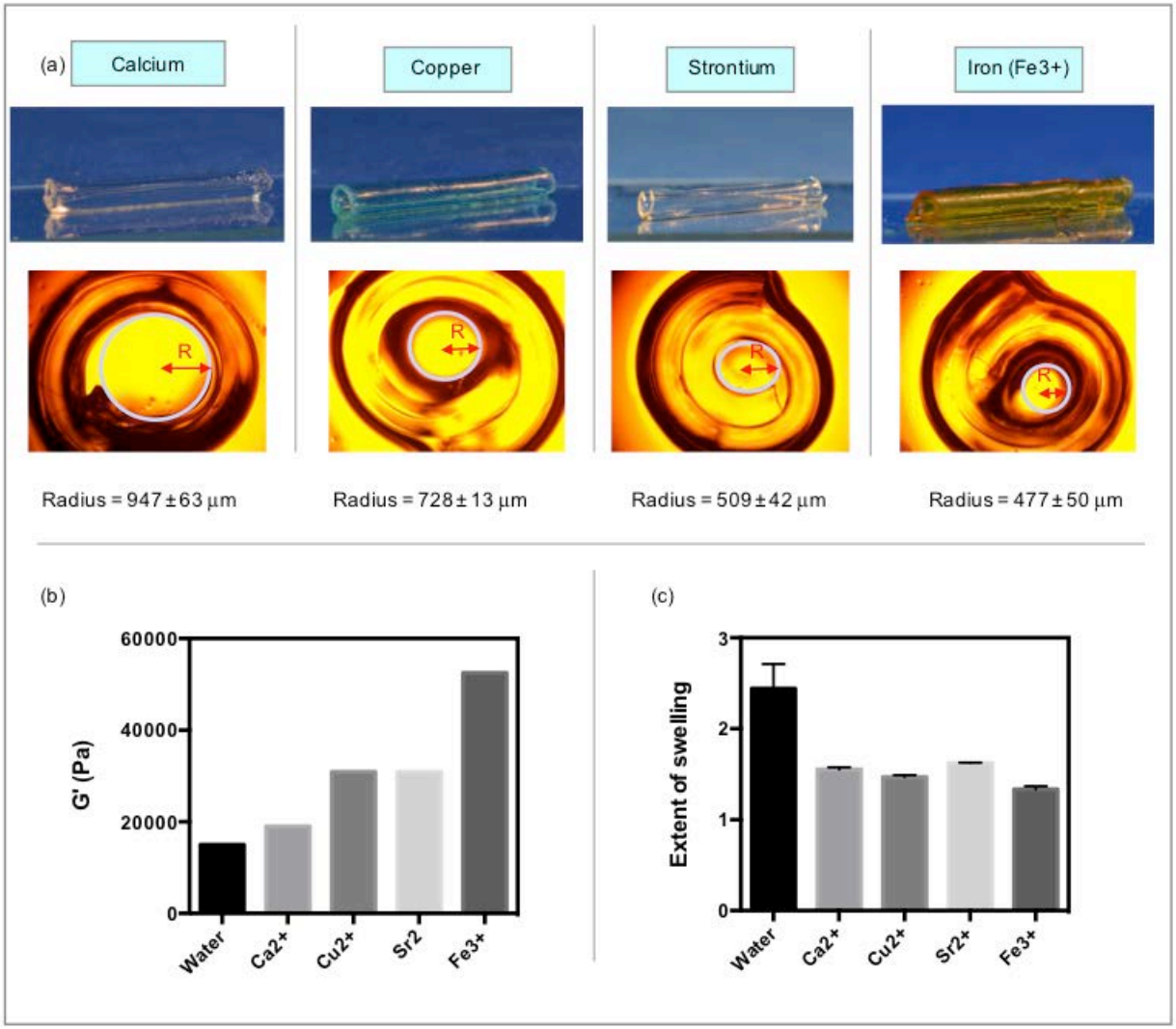

Figure 5.3. (a) Effect of cation type on A/B bilayer gel folding (b) Gel A modulus after crosslinking with different cations. (c) The extent of swelling (swelling ratio) of Gel A following crosslinking with different cations. Error bars are standard deviations from 3 measurements.

We studied several cations for their effect on the folding of A/B bilayer gels. A clear correlation was found in that the cations that induced folding were the same ones that are known to crosslink alginate. These include several multivalent cations, as shown in Figure 5.3. On the other hand, monovalent cations like Na^+ and K^+ as well as the divalent Mg^{2+} did not induce folding, regardless of their concentration. All these are

known to be unable to crosslink alginate. With regard to the cations that do cause folding, the tightness of the fold, i.e., the inner radius of the tube varies with cation type. The results in Figure 5.3 are for 500 mM of the respective salt, and the photos were taken after the structure had reached steady-state. At this concentration, all the gels exhibit long-side folding into tubes, and the inner radius of the tube varies from 947 μm for Ca^{2+} to 447 μm for Fe^{3+}. The outer radius of the tube relatively constant at around 2 mm regardless of the cation.

We can correlate cation effects on folding with the effects of the same cations on gel stiffness. For this, we conducted rheological measurements to measure the gel modulus G' of Gel A (DMAA+ 2 wt% alginate) before and after crosslinking with different cations. The results are shown in Figure 5.3b. G' is ~ 15 kPa when Gel A is in water (i.e., the alginate is not physically crosslinked). Crosslinking with Ca^{2+} increases G' to 20 kPa, while Sr^{2+} and Cu^{2+} give G' ~ 30 kPa, and Fe^{3+} further increases G' to 51 kPa. Thus, the gel stiffness follows the order: $Fe^{3+} > Sr^{2+} \sim Cu^{2+} > Ca^{2+}$. The exact inverse of this pattern is seen for the inner radius of the folded tube, i.e., the stiffer the gel, the tighter the tube. An increase in gel stiffness also inversely correlates with the extent of gel swelling, as shown in Figure 5.3b. The swelling ratio Q is highest when Gel A is in water, i.e., the alginate is uncrosslinked (Q ~ 2.4). Introduction of crosslinking cations decreases the extent of swelling by about 30% (Q ~ 1.6), although the differences between cations are modest. Note that Gel B is unaffected by the presence of cations both in terms of its mechanical properties as well as its extent of swelling. This is to be expected because Gel B is a nonionic gel.

5.3.3 Effect of Ca^{2+} Concentration

So far, we have considered A/B bilayer gels folding at relatively high concentrations of multivalent salts. We now show results for a range of concentrations of one cation, viz. Ca^{2+}. For these experiments, all other conditions were held constant as before: Gel A had 2 wt% of alginate along with DMAA; Gel B had DMAA alone. We found that folding occurs for a wide range of Ca^{2+} concentrations. But the striking result, shown in Figure 5.4, is that folding occurs along the short side for Ca^{2+} of 40 mM and 80 mM, and along the long side for 100 mM and above. Note that the radius of the tube is much higher for the short-side folding cases.

Figure 5.4. Effect of Ca^{2+} concentration on gel folding. The gels demonstrate short-side folding at low concentrations of Ca^{2+} and long-side folding for Ca^{2+} of 100 mM and above.

5.3.4 Effect of Alginate Concentration

Next, we varied the concentration of alginate in Gel A. All other parameters of the gel were identical to those used previously, and folding was studied at 500 mM of Ca^{2+}. The photos in Figure 5.5 were taken at steady state, i.e., there were no further changes in the behavior of the system with time. The photos show that at low alginate concentrations (0.25 wt% and 0.5 wt%), the gel does not fold completely, but it partially bends. However, the bend is along the short-side at 0.25 wt% and along the long side at 0.5 wt%. At concentrations of 1 wt% and higher, the gel shows long-side folding and forms a closed tube.

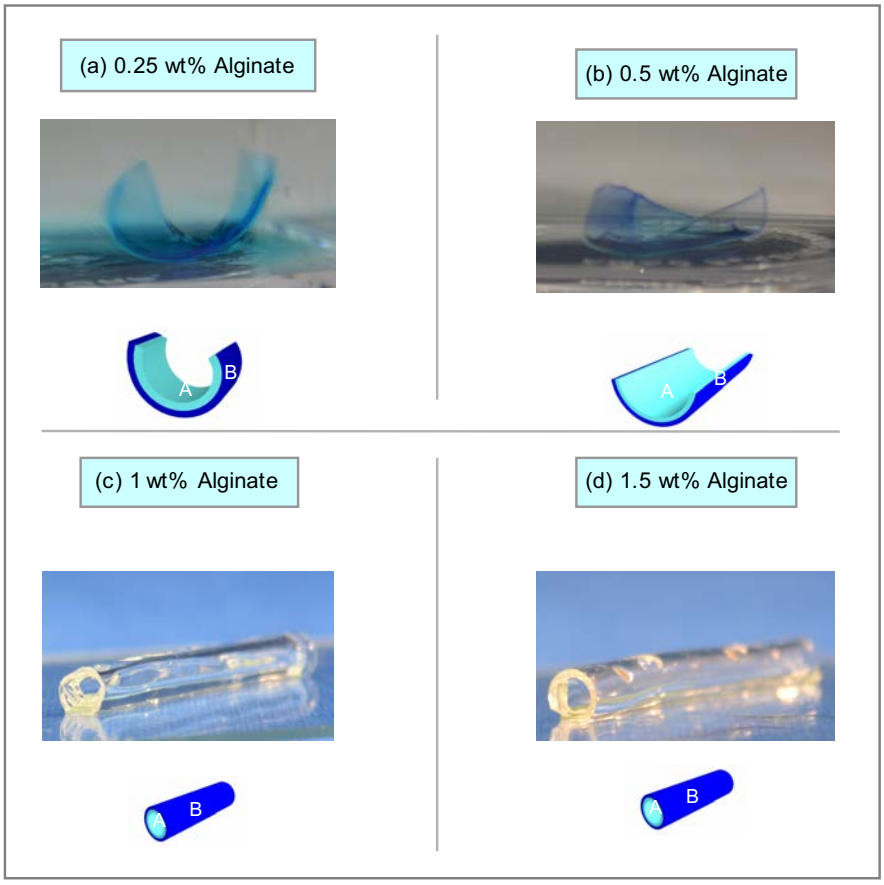

Figure 5.5. Effect of alginate concentration on gel folding. The alginate is included in Gel A along with DMAA. Folding is then studied in 500 mM Ca^{2+}. The gels in (a) and

(b) are dyed blue for clarity. The gel demonstrates short-side partial folding at 0.25 wt%, and long-side partial folding at 0.5 wt%. At higher concentrations the gel folds along its long-side and forms a tube.

5.3.5 Mechanism for Folding

The crucial questions from this study are: (1) why does folding occur at all; and (2) why does it typically occur along the long-side and only in some cases along the short-side. With regard to the first question, our empirical finding is that folding requires the presence of multivalent cations like Ca^{2+} and Fe^{3+} that crosslink the alginate in Gel A. The added crosslinks in Gel A make this layer 2-3 fold stiffer relative to its initial level, and concomitantly, the denser network of Gel A shrinks by about 30% (Figure 5.3). Gel B is unaffected by the same cations. Overall, there is not a huge mismatch between the two layers of the A/B gel in terms of either the mechanical or swelling properties. But perhaps the selective stiffening and shrinking of Gel A (but not Gel B), still creates stresses in the overall rectangular sheet that drive it to fold. Our findings show a consistent pattern in that the shrunken layer of Gel A forms the interior of the tube while the unperturbed layer of Gel B forms the exterior. In our previous studies also (Chapters 3 and 4), the more swollen layer faced the outside and the less swollen one the inside.

Next comes the question regarding the axis of folding. As noted, ours is the first example of long-side folding in freely-swelling gel sheets. This result is observed regardless of the aspect ratio of the sheet. Our experiments show that long-side folding requires high concentrations of alginate in the gel as well as of the crosslinking cations outside the gel. This is an important observation, and it suggests that the strong and rapid binding of the alginate chains to the cations is necessary for the folding of the gel. In

other words, the kinetics of the alginate/Ca^{2+} binding are as important as the thermodynamics of this interaction.

Two ancillary experiments bring out these points further. First, we allowed a gel to partially fold along its short-side in 40 mM Ca^{2+}, and then increased the Ca^{2+} to 500 mM. The gel continued to fold along its short-side, even though the expected behavior at 500 mM Ca^{2+} is to fold along the long-side. This shows that the initial kinetics matter and that gel folding is a nonequilibrium process. In a second experiment, we incubated a gel in a chelated form of calcium, i.e., Ca-EDTA, and then added GdL, which is a slow-releasing acid. As the acid contacts the chelator, Ca^{2+} is released. We chose our conditions such that the total Ca^{2+} released would be ~ 500 mM. Yet, this gel folded along its short-side. This experiment shows that if the initial kinetics of alginate-cation contact are not rapid enough, the preferred pathway is to fold along the short-side. Conversely, rapid kinetics facilitates long-side folding.

Even if rapid kinetics are a must, it still does not explain why the gel folds along its long side. For this, we hypothesize that the cation-induced crosslinking of the Gel A layer is not homogeneous; rather, we suggest that the cations diffuse preferentially along the edges of the rectangular sheet. If so, the edges of the Gel A layer will become stiff before the interior of this layer, and then the edges could act as constraints during the onset of folding. Either the longer edges of the rectangular sheet or the shorter edges will have to bend to permit folding of the sheet. The longer edges will pose a more stringent constraint due to their higher length, and therefore the shorter edges will bend first, and if

so, the sheet will fold about its long-side. Thus, we explain long-side folding as arising due to edge effects, i.e., the stiffening of the edges of the gel sheet. It is only if the kinetics are rapid that such stiffening would occur. Slow kinetics will lead to homogeneous crosslinking of Gel A, and if so, folding of the A/B bilayer will occur along the short side.

5.4 Conclusions

We have studied the shape change of an A/B bilayer gel induced by multivalent cations such as Ca^{2+}. One layer of this gel contains the biopolymer alginate. In the presence of Ca^{2+} ions, the alginate chains get crosslinked and so this layer stiffens and shrinks. In the process, the gel converts from a flat sheet to a folded tube, typically folded along its long-side. Such folding requires a sufficient concentration of both alginate and the cations, which suggests that it is a kinetically driven nonequilibrium effect. We hypothesize that long-side folding is facilitated by inhomogeneous crosslinking that occurs preferentially along the edges of the sheet. The insights gained from this study may be useful in directing the folding of other gel structures.

Chapter 6

Conclusions and Recommendations

6.1 Project Summary and Principal Contributions

In this dissertation, we have shown three different kinds of hybrid gels that undergo a shape transformation in response to a specific trigger. We derived inspiration from the morphological changes exhibited by plants in nature to design our hydrogel structures. The folding of hydrogel bilayers mimics the actuation mechanism in plants. All hybrid gels were prepared with commercially available chemicals and with minimal synthesis. The gels developed in this study responded to a molecular trigger, i.e. MMP-triggered shape transformations in Chapter 3, glucose-triggered self-folding in Chapter 4 and multivalent ion-triggered shape transformations in Chapter 5. The advantage of these molecular triggers is that their reactions are highly specific.

In Chapter 3, we describe hybrid gels that undergo self-folding in response to the presence of physiological concentrations of MMPs. The hybrid gels were fabricated via photolithographic techniques. We used photopatterning to spatially arrange regions of biopolymer that are sensitive to MMPs. Initially, the gel is flat in water due to the stiffness of one of the layers. The degradation of these biopolymer regions leads to a reduction in stiffness. As a result, the flat sheet folds. This is the first time a fully polymeric hydrogel structure was developed to undergo a shape transformation in response to a bimolecular trigger.

In Chapter 4, we reported the fabrication of a bilayer gel that could be used be used to detect the presence of glucose. The hybrid gel was fabricated by sequential UV polymerization. The enzymes were embedded in the passive layer because it does not undergo an increase in swelling. Therefore, it minimizes the diffusion of the enzyme into the solution. This shape transformation is specific and does not occur in the presence of other small sugars. Note, this folding behavior is also reversible, i.e. the folded gel flattens out when returned to water. As a result, these gels are reusable. The kinetics of folding are also dependent on the concentration of glucose. Furthermore, the materials used in this study are biocompatible.

In Chapter 5, we explored the use of multivalent ions as a trigger for self-folding. Our bilayer gel consisted of two layers: (1) dimethylacrylamide (DMAA) (the passive layer) and (2) dimethylacrylamide and alginate (the active layer). The gels folded in the presence of specific multivalent ions such as Ca^{2+}, Fe^{3+} and Cu^{2+}. During this study, we observed that the gels demonstrated long-side folding under certain conditions. This is in contrast to previous studies in the literature, where freely swelling bilayer gels (without patterns on their surface) demonstrate short-side folding. Previous studies that have observed long-side folding involved constraining the hydrogel bilayer to induce long-side folding. The insight gained from this study could be utilized to direct the folding of hydrogel sheets.

We believe that the above studies will find a range of applications due to a change at the molecular level being amplified to a macroscopic change and the ease of fabrication.

6.2 Recommendations for Future Work

The concepts that we have reported in this dissertation can be extended to explore new applications and utilities. Herein, we briefly describe the outline for the future work.

6.2.1 Self-Folding Gels as a Tissue Scaffold

Commonly used techniques for fabrication of tissue scaffolds require the use of specialized equipment that is not widely available. The fabrication of tissue scaffolds can be classified as top-down or bottom-up. The 3D scaffold is first fabricated in the conventional top-down approach. Cells are then seeded on the scaffold. However, the drawback of this method is that the cells are not seeded homogeneously and the cells are typically attached on the edges of the scaffold. The bottom-up approach refers to the process where smaller building blocks are used to create larger structures. This approach is also favored by natural tissues. For example, assemblies in the human body, such as nephrons in a kidney or the bundles of myofibers in muscles consist of repeating functional units. The seeding of cells in a self-folding hydrogel is a better mimic of the process in nature. The advantage of hydrogels is their similarity to biological tissue and there is a range of hydrogels that have been approved for use in medicine. Chemical modification also allows the strucutres to be made more biocompatible. Photolithography also allows us to precisely pattern materials of different stiffness and topographical features.

Cells can be homogeneously seeded within our gels, which is difficult to achieving "top-down" techniques. The homogenously seeded gel can then be fabricated and triggered to fold into a pre-programmed structure by using a MMP or an ion such as Ca^{2+}. These molecular stimuli can also be utilized to induce folding at physiological conditions. Our triggers are milder in comparison to other stimuli such as pH or temperature, which may damage the cells. Furthermore, the use of a biomolecule also ensures specificity. We demonstrate the possibility of encapsulating genetically engineered fluorescent bacteria in our hybrid gels from Chapter 5. Green fluorescent *E. coli* were encapsulated in the DMAA layer, while red fluorescent *E. coli* were encapsulated in the DMAA-Alginate layer. The bacteria were first mixed with the precursor solution. The precursor solutions were then polymerized sequentially using UV light. We examined the gels utilizing fluorescence microscopy to determine the viability of the encapsulated bacteria. We saw that the bacteria were fluorescent in both layers indicating that the *E. coli* was not negatively impacted by UV polymerization. The insights gained from our studies can also be utilized to tune the inner diameter of the final tube.

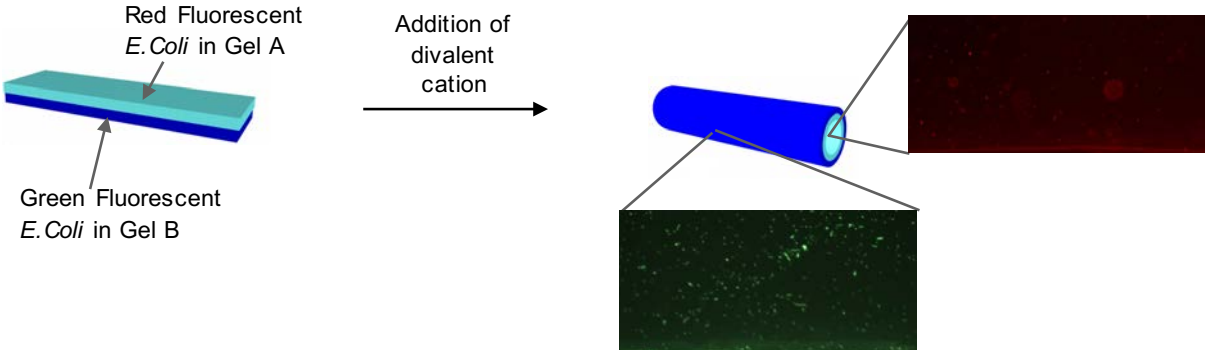

Figure 6.1. Fluorescent *E.Coli* embedded in bilayer hybrid gels of DMAA (Layer A) and DMAA-Alginate (Layer B. Green fluorescent *E.Coli* were embedded in layer A and red fluorescent E.Coli were embedded in layer B. The images show that the cells remained viable after polymerization.

In addition, the use of gelatin (hybrid gels from Chapter 4) is advantageous because of its biocompatibility. Mammalian cells can bind to the Arg-Gly-Asp (RGD) sequence and these cells are also capable of degrading gelatin.[57] These features allow cells to proliferate and migrate into the gel structure, allowing "3D" cell culture. Cells, such as mouse fibroblast cells (L929 cells) can also be seeded on the hybrid gels that were utilized in Chapter 4. These cells secrete MMPs.[63] As a result, the gel would start to fold as the cells proliferate and the regions containing gelatin are degraded.

6.2.2 Fabrication of Complex Structures

Our plan for future work for the fabrication of shape-morphing gels is to fabricate architectures in 3D. Most shape-changing gels are fabricated in 2D and an external trigger such as pH or temperature is used to induce self-folding.[11] However, in order to expand these applications of these gels, it is necessary to fabricate structures in 3D that have the ability to form other complex structures. This would allow us to better mimic the shape changes exhibited by plants.

Recently, our lab developed a technique for fabricating hybrid gels by utilizing monomer solutions with sufficiently high viscosity.[52] The high viscosities reduce the effect of diffusion at the common gel interface. These high viscosity solutions were utilized to create gels with distinct regions of differing mechanical properties. For example, a gel with elastic and brittle regions can be incorporated into a hybrid structure

that is divided by a sharp interface. We believe that this technique can be used in conjunction with a homemade 3D printer to fabricate structures in 3D. The homemade 3D printer would consist of a syringe pump and computer-controlled three-axis stage. The viscosities of the solutions can be tuned by using clays such as laponite or biopolymers such as xanthan gum. UV polymerization can be used to sequentially cure each layer. We believe that technique would allow us to precisely program different structures.

References:

[1] Elbaum, R.; Gorb, S.; Fratzl, P. "Structures in the cell wall that enable hygroscopic movement of wheat awns." *J. Struct. Biol.* **2008**, *164*, 101-107.

[2] Armon, S.; Efrati, E.; Kupferman, R.; Sharon, E. "Geometry and mechanics in the opening of chiral seed pods." *Science* **2011**, *333*, 1726-1730.

[3] Tanaka, T. "Gels." *Sci. Am.* **1981**, *244*, 124.

[4] Osada, Y.; Ping Gong, J.; Tanaka, Y. "Polymer gels." *J Macromol. Sci. C* **2004**, *44*, 87-112.

[5] White, E. M.; Yatvin, J.; Grubbs, J. B.; Bilbrey, J. A.; Locklin, J. "Advances in smart materials: Stimuli−responsive hydrogel thin films." *J. Polym. Sci. Part B Polym. Phys.* **2013**, *51*, 1084-1099.

[6] Ahn, S.-k.; Kasi, R. M.; Kim, S.-C.; Sharma, N.; Zhou, Y. "Stimuli-responsive polymer gels." *Soft Matter* **2008**, *4*, 1151-1157.

[7] Hu, Z.; Zhang, X.; Li, Y. "Synthesis and application of modulated polymer gels." *Science* **1995**, *269*, 525-527.

[8] Guan, J.; He, H.; Hansford, D. J.; Lee, L. J. "Self-folding of three-dimensional hydrogel microstructures." *J. Phys. Chem. B* **2005**, *109*, 23134-23137.

[9] Techawanitchai, P.; Ebara, M.; Idota, N.; Asoh, T.-A.; Kikuchi, A.; Aoyagi, T. "Photo-switchable control of pH-responsive actuators via pH jump reaction." *Soft Matter* **2012**, *8*, 2844-2851.

[10] Shim, T. S.; Kim, S. H.; Heo, C. J.; Jeon, H. C.; Yang, S. M. "Controlled origami folding of hydrogel bilayers with sustained reversibility for robust microcarriers." *Angew. Chem. Int. Ed.* **2012**, *124*, 1449-1452.

[11] Ionov, L. "Biomimetic Hydrogel-Based Actuating Systems." *Adv. Mater.* **2013**, *23*, 4555-4570.

[12] Gracias, D. H. "Stimuli responsive self-folding using thin polymer films." *Curr. Opin. Chem. Eng.* **2013**, *2*, 112-119.

[13] Yu, Q.; Bauer, J. M.; Moore, J. S.; Beebe, D. J. "Responsive biomimetic hydrogel valve for microfluidics." *Appl. Phys. Lett* **2001**, *78*, 2589-2591.

[14] Fernandes, R.; Gracias, D. H. "Self-folding polymeric containers for encapsulation and delivery of drugs." *Adv. Drug Delivery Rev.* **2012**, *64*, 1579-1589.

[15] Bassik, N.; Brafman, A.; Zarafshar, A. M.; Jamal, M.; Luvsanjav, D.; Selaru, F. M.; Gracias, D. H. "Enzymatically triggered actuation of miniaturized tools." *J. Am. Chem. Soc.* **2010**, *132*, 16314-16317.

[16] Stoychev, G.; Puretskiy, N.; Ionov, L. "Self-folding all-polymer thermoresponsive microcapsules." *Soft Matter* **2011**, *7*, 3277-3279.

[17] Bassik, N.; Abebe, B. T.; Laflin, K. E.; Gracias, D. H. "Photolithographically patterned smart hydrogel based bilayer actuators." *Polymer* **2010**, *51*, 6093-6098.

[18] Alberts, B. *Molecular biology of the cell*; Garland Science: New York, 2008.

[19] Burdick, J. A.; Murphy, W. L. "Moving from static to dynamic complexity in hydrogel design." *Nat. Commun.* **2012**, *3*, 1269.

[20] Alben, S.; Balakrisnan, B.; Smela, E. "Edge effects determine the direction of bilayer bending." *Nano Lett.* **2011**, *11*, 2280-2285.

[21] Incorvaia, L.; Badalamenti, G.; Rini, G.; Arcara, C.; Fricano, S.; Sferrazza, C.; Di Trapani, D.; Gebbia, N.; Leto, G. "MMP-2, MMP-9 and activin A blood levels in patients with breast cancer or prostate cancer metastatic to the bone." *Anticancer Res.* **2007**, *27*, 1519-1525.

[22] Fairbanks, B. D.; Schwartz, M. P.; Bowman, C. N.; Anseth, K. S. "Photoinitiated polymerization of PEG-diacrylate with lithium phenyl-2, 4, 6-trimethylbenzoylphosphinate: polymerization rate and cytocompatibility." *Biomaterials* **2009**, *30*, 6702-6707.

[23] Schild, H. G. "Poly (N-isopropylacrylamide): experiment, theory and application." *Prog. Polym. Sci.* **1992**, *17*, 163-249.

[24] Beltran, S.; Baker, J. P.; Hooper, H. H.; Blanch, H. W.; Prausnitz, J. M. "Swelling equilibria for weakly ionizable, temperature-sensitive hydrogels." *Macromolecules* **1991**, *24*, 549-551.

[25] Haraguchi, K.; Takehisa, T. "Nanocomposite hydrogels: a unique organic-inorganic network structure with extraordinary mechanical, optical, and swelling/de-swelling properties." *Adv. Mater.* **2002**, *14*, 1120.

[26] Klouda, L.; Mikos, A. G. "Thermoresponsive hydrogels in biomedical applications." *Eur. J. Pharm. Biopharm.* **2008**, *68*, 34-45.

[27] Hirokawa, Y.; Tanaka, T. "Volume phase transition in a nonionic gel." *J. Chem. Phys.* **1984**, *81*, 6379-6380.

[28] Hu, X.; Li, D.; Zhou, F.; Gao, C. “On the structure alteration of crosslinkable gelatin coupled with methacrylic acid and its hydrogel.” *e-Polymers* **2012**, *12*, 151-159.

[29] Mookhtiar, K.; Van Wart, H. “Clostridium histolyticum collagenases: a new look at some old enzymes.” *Matrix* **1991**, *1*, 116-126.

[30] Pawar, S. N.; Edgar, K. J. “Alginate derivatization: a review of chemistry, properties and applications.” *Biomaterials* **2012**, *33*, 3279-3305.

[31] Augst, A. D.; Kong, H. J.; Mooney, D. J. “Alginate hydrogels as biomaterials.” *Macromol. Biosci.* **2006**, *6*, 623-633.

[32] Dunlop, J. W.; Weinkamer, R.; Fratzl, P. “Artful interfaces within biological materials.” *Mater. Today* **2011**, *14*, 70-78.

[33] Holmes, D. P.; Crosby, A. J. “Snapping surfaces.” *Adv. Mater* **2007**, *19*, 3589-3593.

[34] Dawson, C.; Vincent, J. F.; Rocca, A.-M. “How pine cones open.” *Nature* **1997**, *390*, 668-668.

[35] Forterre, Y.; Skotheim, J. M.; Dumais, J.; Mahadevan, L. “How the Venus flytrap snaps.” *Nature* **2005**, *433*, 421-425.

[36] Timoshenko, S. “Analysis of bi-metal thermostats.” *J. Opt. Soc. Am* **1925**, *11*, 233-255.

[37] Kim, J.; Hanna, J. A.; Byun, M.; Santangelo, C. D.; Hayward, R. C. “Designing responsive buckled surfaces by halftone gel lithography.” *Science* **2012**, *335*, 1201-1205.

[38] Wu, Z. L.; Moshe, M.; Greener, J.; Therien-Aubin, H.; Nie, Z.; Sharon, E.; Kumacheva, E. “Three-dimensional shape transformations of hydrogel sheets induced by small-scale modulation of internal stresses.” *Nat. Commun.* **2013**, *4*, 1586.

[39] Ahn, S. K.; Kasi, R. M.; Kim, S. C.; Sharma, N.; Zhou, Y. X. “Stimuli-Responsive Polymer Gels.” *Soft Matter* **2008**, *4*, 1151-1157.

[40] White, E. M.; Yatvin, J.; Grubbs, J. B.; Bilbrey, J. A.; Locklin, J. “Advances in Smart Materials: Stimuli-Responsive Hydrogel Thin Films.” *J. Polym. Sci., Part B: Polym. Phys.* **2013**, *51*, 1084-1099.

[41] Cipriano, B. H.; Banik, S. J.; Sharma, R.; Rumore, D.; Hwang, W.; Briber, R. M.; Raghavan, S. R. "Superabsorbent hydrogels that are robust and highly stretchable." *Macromolecules* **2014**, *47*, 4445-4452.

[42] Kempaiah, R.; Nie, Z. H. "From nature to synthetic systems: Shape transformation in soft materials." *J. Mat. Chem. B* **2014**, *2*, 2357-2368.

[43] Liu, Y.; Genzer, J.; Dickey, M. D. ""2D or not 2D": Shape-programming polymer sheets." *Prog. Polym. Sci.* **2016**, *52*, 79-106.

[44] Thérien-Aubin, H.; Wu, Z. L.; Nie, Z.; Kumacheva, E. "Multiple shape transformations of composite hydrogel sheets." *J. Am. Chem. Soc.* **2013**, *135*, 4834-4839.

[45] Wei, Z. J.; Jia, Z.; Athas, J. M.; Wang, C. Y.; Raghavan, S. R.; Li, T.; Nie, Z. H. "Hybrid hydrogel sheets that undergo pre-programmed shape transformations." *Soft Matter* **2014**, *10*, 8157-8162.

[46] Hodick, D.; Sievers, A. "On the Mechanism of Trap Closure of Venus Flytrap (*Dionaea Muscipula* Ellis)." *Planta* **1989**, *179*, 32-42.

[47] Markin, V. S.; Volkov, A. G.; Jovanov, E. "Active Movements in Plants: Mechanism of Trap Closure by *Dionaea Muscipula* Ellis." *Plant Signaling Behav.* **2008**, *3*, 778-783.

[48] Volkov, A. G.; Adesina, T.; Markin, V. S.; Jovanov, E. "Kinetics and Mechanism of *Dionaea Muscipula* Trap Closing." *Plant Physiol.* **2008**, *146*, 694-702.

[49] Burgert, I.; Fratzl, P. "Actuation Systems in Plants as Prototypes for Bioinspired Devices." *Philos. Trans. R. Soc., A* **2009**, *367*, 1541-1557.

[50] Poppinga, S.; Masselter, T.; Speck, T. "Faster Than Their Prey: New Insights into the Rapid Movements of Active Carnivorous Plants Traps." *Bioessays* **2013**, *35*, 649-657.

[51] Palleau, E.; Morales, D.; Dickey, M. D.; Velev, O. D. "Reversible Patterning and Actuation of Hydrogels by Electrically Assisted Ionoprinting." *Nat. Commun.* **2013**, *4*, 2257.

[52] Banik, S. J.; Fernandes, N. J.; Thomas, P. C.; Raghavan, S. R. "A new approach for creating polymer hydrogels with regions of distinct chemical, mechanical, and optical properties." *Macromolecules* **2012**, *45*, 5712-5717.

[53] Byrne, M. E.; Park, K.; Peppas, N. A. "Molecular imprinting within hydrogels." *Adv. Drug Deliv. Rev.* **2002**, *54*, 149-161.

[54] Miyata, T.; Uragami, T.; Nakamae, K. "Biomolecule-sensitive hydrogels." *Adv. Drug Deliv. Rev.* **2002**, *54*, 79-98.

[55] Alberts, B. *Molecular Biology of the Cell*; Garland Publishers: New York, 2002.

[56] Klein, Y.; Efrati, E.; Sharon, E. "Shaping of elastic sheets by prescription of non-Euclidean metrics." *Science* **2007**, *315*, 1116-1120.

[57] Nichol, J. W.; Koshy, S. T.; Bae, H.; Hwang, C. M.; Yamanlar, S.; Khademhosseini, A. "Cell-laden microengineered gelatin methacrylate hydrogels." *Biomaterials* **2010**, *31*, 5536-5544.

[58] Brinkman, W. T.; Nagapudi, K.; Thomas, B. S.; Chaikof, E. L. "Photo-cross-linking of type I collagen gels in the presence of smooth muscle cells: mechanical properties, cell viability, and function." *Biomacromolecules* **2003**, *4*, 890-895.

[59] Haraguchi, K. "Stimuli-responsive nanocomposite gels." *Colloid Polym. Sci.* **2011**, *289*, 455-473.

[60] Birkedal-Hansen, H.; Moore, W.; Bodden, M.; Windsor, L.; Birkedal-Hansen, B.; DeCarlo, A.; Engler, J. "Matrix metalloproteinases: a review." *Crit. Rev. Oral. Biol. M.* **1993**, *4*, 197-250.

[61] Djabourov, M. "Architecture of gelatin gels." *Contemp. Phys.* **1988**, *29*, 273-297.

[62] Macosko, C. W. *Rheology: Principles, Measurements, and Applications*; Wiley-VCH: New York, 1994.

[63] McAnulty, R. J. "Fibroblasts and myofibroblasts: their source, function and role in disease." *Int. J. Biochem. Cell. B* **2007**, *39*, 666-671.

[64] Hashimoto, M.; Yamaguchi, S.; Sasaki, J. I.; Kawai, K.; Kawakami, H.; Iwasaki, Y.; Imazato, S. "Inhibition of Matrix Metalloproteinases and Toxicity of Gold and Platinum Nanoparticles in L929 Fibroblast Cells." *Eur. J. Oral Sci.* **2016**, *124*, 68-74.

[65] Raba, J.; Mottola, H. A. "Glucose oxidase as an analytical reagent." *Crit. Rev. Anal. Chem.* **1995**, *25*, 1-42.

[66] O'malley, J. J.; Ulmer, R. W. "Thermal stability of glucose oxidase and its admixtures with synthetic polymers." *Biotechnol. Bioeng.* **1973**, *15*, 917-925.

[67] Heller, A.; Feldman, B. "Electrochemistry in diabetes management." *Acc. Chem. Res.* **2010**, *43*, 963-973.

[68] Newman, J. D.; Turner, A. P. "Home blood glucose biosensors: a commercial perspective." *Biosens. Bioelectron.* **2005**, *20*, 2435-2453.

[69] Rumley, A. "Urine dipstick testing: comparison of results obtained by visual reading and with the Bayer CLINITEK 50." *Ann. Clin. Biochem.* **2000**, *37*, 220-221.

[70] Traitel, T.; Cohen, Y.; Kost, J. "Characterization of glucose-sensitive insulin release systems in simulated in vivo conditions." *Biomaterials* **2000**, *21*, 1679-1687.

[71] Liu, Y.; Javvaji, V.; Raghavan, S. R.; Bentley, W. E.; Payne, G. F. "Glucose oxidase-mediated gelation: a simple test to detect glucose in food products." *J. Agric. Food Chem.* **2012**, *60*, 8963-8967.

[72] Jung, D.-Y.; Magda, J. J.; Han, I. S. "Catalase effects on glucose-sensitive hydrogels." *Macromolecules* **2000**, *33*, 3332-3336.

[73] Ottenbrite, R. M.; Kim, S. W. *Polymeric drugs and drug delivery systems*; CRC Press, 2000.

[74] Kleppe, K. "The Effect of Hydrogen Peroxide on Glucose Oxidase from Aspergillus niger*." *Biochemistry* **1966**, *5*, 139-143.

[75] Tse, P. H.; Gough, D. A. "Time dependent inactivation of immobilized glucose oxidase and catalase." *Biotechnol. Bioeng.* **1987**, *29*, 705-713.

[76] Gu, Z.; Dang, T. T.; Ma, M.; Tang, B. C.; Cheng, H.; Jiang, S.; Dong, Y.; Zhang, Y.; Anderson, D. G. "Glucose-responsive microgels integrated with enzyme nanocapsules for closed-loop insulin delivery." *ACS nano* **2013**, *7*, 6758-6766.

[77] Gu, Z.; Aimetti, A. A.; Wang, Q.; Dang, T. T.; Zhang, Y.; Veiseh, O.; Cheng, H.; Langer, R. S.; Anderson, D. G. "Injectable nano-network for glucose-mediated insulin delivery." *ACS nano* **2013**, *7*, 4194-4201.

[78] Schneider, C. A.; Rasband, W. S.; Eliceiri, K. W. "NIH Image to ImageJ: 25 years of image analysis." *Nat. Methods* **2012**, *9*, 671-675.

[79] Rubinstein, M.; Colby, R. H. *Polymer physics 2003*.

[80] Erickson, H. P. "Size and shape of protein molecules at the nanometer level determined by sedimentation, gel filtration, and electron microscopy." *Biol. Proced. Online* **2009**, *11*, 32.

[81] Chun, I. S.; Challa, A.; Derickson, B.; Hsia, K. J.; Li, X. "Geometry effect on the strain-induced self-rolling of semiconductor membranes." *Nano Lett.* **2010**, *10*, 3927-3932.

[82] Stoychev, G.; Zakharchenko, S.; Turcaud, S. b.; Dunlop, J. W.; Ionov, L. "Shape-programmed folding of stimuli-responsive polymer bilayers." *ACS nano* **2012**, *6*, 3925-3934.

[83] Hou, M. T.-K.; Chen, R. "Effect of width on the stress-induced bending of micromachined bilayer cantilevers." *J. Micromech. Microeng.* **2002**, *13*, 141.

[84] Gong, J. P. "Why are double network hydrogels so tough?" *Soft Matter* **2010**, *6*, 2583-2590.